

# Thermal cabin model development for interior climate simulations

A co-simulation approach using GT-SUITE and TAITHERM

Master's thesis in Applied mechanics  
Master's thesis in Sustainable Energy Systems

KARTHIKEYAN GNANASUNDARAM

HARIKRISHNAN MURALIDHARAN



MASTER'S THESIS 2023

# Thermal cabin model development for interior climate simulations

A co-simulation approach using GT-SUITE and TAITHERM

KARTHIKEYAN GNANASUNDARAM  
HARIKRISHNAN MURALIDHARAN



**CHALMERS**  
UNIVERSITY OF TECHNOLOGY

Department of Mechanics and Maritime Sciences  
*Division of Vehicle Engineering and Autonomous Systems*  
CHALMERS UNIVERSITY OF TECHNOLOGY  
Gothenburg, Sweden 2023

Thermal cabin model development for interior climate simulations  
A co-simulation approach using GT-SUITE and TAITHERM  
KARTHIKEYAN GNANASUNDARAM  
HARIKRISHNAN MURALIDHARAN

© KARTHIKEYAN GNANASUNDARAM, 2023.  
© HARIKRISHNAN MURALIDHARAN, 2023.

Supervisor: Hannes Karlsson, Volvo Car Corporation  
Examiner: Alexey Vdovin, Department of Mechanics and Maritime Sciences

Master's Thesis 2023  
Department of Mechanics and Maritime Sciences  
Division of Vehicle Engineering and Autonomous Systems  
Chalmers University of Technology  
SE-412 96 Gothenburg  
Telephone +46 31 772 1000

Cover: Different attributes involved in the co-simulation process

Typeset in L<sup>A</sup>T<sub>E</sub>X  
Printed by Chalmers Reproservice  
Gothenburg, Sweden 2023

Thermal cabin model development for interior climate simulations  
A co-simulation approach using GT-Suite and TAITherm  
KARTHIKEYAN GNANASUNDARAM  
HARIKRISHNAN MURALIDHARAN  
Department of Mechanics and Maritime Sciences  
Chalmers University of Technology

## Abstract

With the increased focus on electric vehicles, decreasing the energy consumption of the climate system is becoming increasingly important. In order to achieve that, a thermal model of the car cabin that can predict the temperature at different zones in the cabin accurately is highly desired. The model should be able to predict the cabin temperature for different ambient conditions as well as different HVAC conditions.

The thesis focuses on developing such a model and analysing the results by comparing them with experimental data. A co-simulation methodology developed by Gamma Technology was used where the fluid domain in the cabin was solved by GT-Suite and the temperature of the cabin wall structures was solved by TAITherm. These models exchange data at prescribed communication intervals so that the thermal features in the cabin can be captured accurately. The model needed to be calibrated against experimental data by using a Heat Transfer Coefficient Multiplier (HTCM). To increase the accuracy of the solution and to eliminate the need for calibration, an extension of this method where CFD data from steady-state simulations carried out in Star CCM+ were mapped onto the co-simulation model. The results from both methods were compared with the experimental data and have been discussed in detail in this thesis.

Keywords: cabin model, co-simulation, CFD, climate system, HVAC, heat transfer, GT-Suite, TAITherm, Star CCM+



## Acknowledgements

We would like to thank our supervisor Hannes Karlsson for his constant support and guidance throughout this project. We also would like to Christoph Boettcher and the support team at Gamma Technologies for helping us through the technical details of the project. Additionally, we want to thank the support team at Thermoanalytics for their support. We would like to express gratitude to our manager Linda Stridsberg and the entire Climate CAE team at Volvo Car Corporation. A special thanks to Alexey Vdovin for being our examiner and guiding us through the process.

Lastly, we would like to thank our families for their encouragement and support they have shown at every step in our lives.

Karthikeyan Gnanasundaram and Harikrishnan Muralidharan,  
Gothenburg, June 2023



# List of Acronyms

Below is the list of acronyms that have been used throughout this thesis listed in alphabetical order:

CAD	Computer Aided Design
CFD	Computational Fluid Dynamics
GT	Gamma Technologies
HTC	Heat Transfer Coefficient
HTCM	Heat Transfer Coefficient Multiplier
HVAC	Heating Ventilation and Air Conditioning
IC	Internal Combustion
RANS	Reynolds Averaged Navier Stokes
RPM	Rotations per minute



# Contents

<b>List of Acronyms</b>	<b>ix</b>
<b>List of Figures</b>	<b>xiii</b>
<b>List of Tables</b>	<b>xv</b>
<b>1 Introduction</b>	<b>1</b>
1.1 Background . . . . .	1
1.2 Aim . . . . .	1
1.3 Limitations . . . . .	2
<b>2 Theory</b>	<b>3</b>
2.1 Fluid Mechanics . . . . .	3
2.1.1 Governing equations . . . . .	3
2.1.1.1 Continuity equation . . . . .	3
2.1.1.2 Momentum equation . . . . .	3
2.1.1.3 Energy equation . . . . .	4
2.1.2 Turbulence modelling . . . . .	4
2.1.2.1 The $k - \epsilon$ turbulence model . . . . .	4
2.2 Heat Transfer . . . . .	5
2.2.1 Conduction . . . . .	5
2.2.2 Convection . . . . .	6
2.2.3 Radiation . . . . .	6
2.2.4 Dimensionless numbers . . . . .	6
2.2.4.1 Nusselt Number . . . . .	7
2.2.4.2 Grashof Number . . . . .	7
2.2.4.3 Prandtl Number . . . . .	7
2.2.4.4 Reynolds Number . . . . .	8
2.3 Co-Simulation . . . . .	8
<b>3 Methods</b>	<b>9</b>
3.1 GT-Flow Solution . . . . .	9
3.1.1 Co-Simulation with GT-Suite and TAItherm . . . . .	9
3.1.2 Mesh Mapping . . . . .	10
3.1.3 Communication interval . . . . .	11
3.1.4 Work Process in GT-Flow Solution . . . . .	12
3.1.4.1 Pre-processing and Meshing in ANSA . . . . .	13

3.1.4.2	Model Building in COOL 3D . . . . .	13
3.1.4.3	TAITherm model . . . . .	15
3.1.4.4	System simulation setup in GT-ISE . . . . .	16
3.2	CFD flow field mapping . . . . .	17
3.2.1	Set up in Star CCM+ . . . . .	18
3.2.2	Discretization in COOL3D . . . . .	20
3.3	Heat-up test setup . . . . .	21
3.4	Sensor positioning . . . . .	23
<b>4</b>	<b>Results and Discussion</b>	<b>25</b>
4.1	TAITherm mesh study . . . . .	25
4.2	GT-Flow Solution . . . . .	27
4.2.1	Results without calibration . . . . .	27
4.2.2	Results with calibration . . . . .	31
4.2.3	Flow cube size variation . . . . .	34
4.3	GT Solution with CFD flow field mapping . . . . .	36
4.3.1	3D CFD Maps . . . . .	36
4.3.2	Results with 3D CFD Mapping . . . . .	39
4.4	Comparison of GT-Flow Solution and CFD Mapping Solution . . . . .	42
4.4.1	Temperature distribution . . . . .	42
4.4.2	Computational time . . . . .	44
<b>5</b>	<b>Conclusion</b>	<b>47</b>
<b>6</b>	<b>Future works</b>	<b>49</b>
	<b>Bibliography</b>	<b>51</b>

# List of Figures

3.1	Representation of data exchange between GT-Suite and TAITherm models . . . . .	10
3.2	Representation of mesh mapping between GT-Suite and TAITherm . . . . .	11
3.3	Time steps and communication intervals used in the co-simulation model . . . . .	12
3.4	Flow chart of the work process for GT-Flow Solution . . . . .	12
3.5	Meshed model in ANSA . . . . .	13
3.6	Flow space defined in COOL3D . . . . .	14
3.7	Discretized flow space in COOL3D . . . . .	14
3.8	TAITherm model . . . . .	15
3.9	System simulation setup in GT-ISE . . . . .	16
3.10	Process flow when CFD flow field mapping is used . . . . .	17
3.11	Cross sectional side view of the meshed geometry . . . . .	18
3.12	Cross sectional top view of the meshed geometry . . . . .	19
3.13	Prism layers in the mesh . . . . .	19
3.14	Discretized flow space in COOL3D using the mesh file from Star CCM+ . . . . .	21
3.15	Different fan speeds . . . . .	22
3.16	Schematic of the cabin with sensor positions . . . . .	23
4.1	Temperature curves of the air node placed inside the cabin for different meshes . . . . .	26
4.2	Number of iterations taken by the solver to compute for 600 time steps in different meshes . . . . .	27
4.3	Comparison of temperature curves from the experiment with the simulation model at the four head positions in the cabin which are (a) Driver (b) Passenger (c) Rear left seat (d) Rear right seat . . . . .	28
4.4	Comparison of temperature curves from the experiment with the simulation model at the four chest positions in the cabin which are (a) Driver (b) Passenger (c) Rear left seat (d) Rear right seat . . . . .	29
4.5	Comparison of temperature curves from the experiment with the simulation model at the four foot positions in the cabin which are (a) Driver (b) Passenger (c) Rear left seat (d) Rear right seat . . . . .	30
4.6	Average temperature recorded by all the 12 sensors placed in the cabin in experiments and simulation model . . . . .	30
4.7	Average temperature recorded by all the 12 sensors placed in the cabin in experiments and simulation model . . . . .	31

4.8	Comparison of temperature curves from the experiment with the simulation model at the four head positions in the cabin which are (a) Driver (b) Passenger (c) Rear left seat (d) Rear right seat . . . . .	32
4.9	Comparison of temperature curves from the experiment with the simulation model at the four chest positions in the cabin which are (a) Driver (b) Passenger (c) Rear left seat (d) Rear right seat . . . . .	33
4.10	Comparison of temperature curves from the experiment with the simulation model at the four foot positions in the cabin which are (a) Driver (b) Passenger (c) Rear left seat (d) Rear right seat . . . . .	34
4.11	Discretized domain when flow cubes were set to (a) 100x100x100 mm (b) 130x130x130 mm (c) 150x150x150 mm . . . . .	35
4.12	Average temperature recorded by all sensors in the model for a HTCM value of 20 for different flow cube sizes . . . . .	35
4.13	Velocity contour plot at the vent cross section when fan speed was set to level 1 . . . . .	37
4.14	Velocity contour plot at the vent cross section when fan speed was set to level 2 . . . . .	37
4.15	Velocity contour plot at the vent cross section when fan speed was set to level 3 . . . . .	38
4.16	Velocity contour plot at the vent cross section when fan speed was set to level 4 . . . . .	38
4.17	Average temperature recorded by all the 12 sensors placed in the cabin in experiments and simulation model . . . . .	39
4.18	Comparison of temperature curves from the experiment with the simulation model at the four head positions in the cabin which are (a) Driver (b) Passenger (c) Rear left seat (d) Rear right seat . . . . .	40
4.19	Comparison of temperature curves from the experiment with the simulation model at the four chest positions in the cabin which are (a) Driver (b) Passenger (c) Rear left seat (d) Rear right seat . . . . .	41
4.20	Comparison of temperature curves from the experiment with the simulation model at the four foot positions in the cabin which are (a) Driver (b) Passenger (c) Rear left seat (d) Rear right seat . . . . .	42
4.21	Temperature contours in the cabin cross sectional area after 15 minutes of simulation time . . . . .	43
4.22	Temperature contours in the cabin cross sectional area after 30 minutes of simulation time . . . . .	43
4.23	Temperature contours in the cabin cross sectional area after 45 minutes of simulation time . . . . .	43
4.24	Temperature contours in the cabin cross sectional area after 60 minutes of simulation time . . . . .	44
4.25	Computational time for the different simulations . . . . .	45

# List of Tables

3.1	Physics models chosen for the steady state simulations . . . . .	20
3.2	Heat-up test parameters . . . . .	22
4.1	Different meshes tested . . . . .	25
4.2	Description of the simulations for which the computational time was compared . . . . .	45



# 1

## Introduction

### 1.1 Background

With the automotive industry moving towards complete electrification as the primary energy source for the drive system, there is a lot of investment going into research and development for the conversion from traditional IC engine models to electric models. One such area of research is cabin climate simulation and to study how various factors affect the cabin climate in the car.

One such factor that affects the cabin climate is solar load. According to [5], solar load can significantly increase the temperature inside the cabin, especially areas that are directly exposed to the sunlight such as the dashboard, steering wheel and seats. This shows that solar flux inclusion can be important in some cases. However, in colder climatic conditions, the effect of solar load is less. Apart from external factors like solar radiation, internal cabin features like the positioning of the inlet and outlet vents, fan speed in the HVAC and the cabin geometry also has an effect on the air distribution inside the cabin that maintains the cabin temperature [4]. The study [4] provided some valuable insights into the design of an effective ventilation system, adjustable air vents, optimized fan placement and the use of seat and dashboard designs that can facilitate better air circulation.

Another important factor that needs to be considered by car manufacturers is the thermal comfort of the occupants inside the car, i.e. providing a comfortable climate in the cabin for the drivers and passengers. This study [6] uses a combination of thermal comfort models and Computational Fluid Dynamics (CFD) to model the cabin climate that essentially helps in optimizing the energy consumption in the thermal system of the car.

Therefore, it is important to have a high-fidelity thermal model to capture the cabin temperature with reasonable accuracy which could help develop thermal systems with better efficiency.

### 1.2 Aim

This thesis project aims to develop a thermal model of a cabin to simulate the interior climate temperature for various conditions. This model will aim to capture the temperature at points of interest inside the cabin such as driver head position,

passenger head position, driver feet position, passenger feet position, etc. The model will be simulated for a heat-up test and the transient temperature curves will be captured. This is aimed to be done in three steps:

- Develop the model by co-simulation of a 1D software and 3D thermal solver, thereby capturing the heat transfer between the cabin and the atmosphere.
- Increase the accuracy of the model and eliminate the need for calibration by mapping the 3D CFD data into the model.
- Comparing the results of the model with experimental data obtained from a heat-up test performed in the climate wind tunnel and predicting the accuracy of the model developed.

### 1.3 Limitations

Generally, the thermal properties of any model are captured by running a full 3D CFD simulation that is transient in nature. This requires a lot of computational time; hence the proposed method was developed. The major limitation of this method is that the results are not as accurate as that of the full 3D CFD transient simulation. Apart from this, the other minor limitations are.

- Solar loading is not included in the model or the test. The presence of heat from the sun can affect the heat transfer within the car cabin which is not studied here. However, the presence of solar loading will have more impact on a cool-down test than a heat-up test.
- Other climatic phenomenon such as the presence of rain or snow and how that affects the cabin condition is not investigated in this thesis.
- Human mannequin modelling, i.e. the presence of a human body inside the cabin and its effect on the cabin temperature is not included in this model.

# 2

## Theory

### 2.1 Fluid Mechanics

Fluid mechanics deals with the study of fluids in rest and motion. Computational Fluid Dynamics (CFD) is the technique of solving a system of equations that govern a fluid flow. These systems can involve equations from fluid dynamics, heat transfer and even chemical reactions.

#### 2.1.1 Governing equations

Governing equations form the basis for Computational Fluid Dynamics (CFD). These equations govern the fluid motion and therefore need to be solved numerically in order to simulate any fluid flow in a CFD software. These equations are in differential form, therefore certain approximations and assumptions are generally used while solving them using numerical methods. There are three main equations, namely continuity, momentum and energy equations which are discussed in detail. The governing equations in CFD are mathematical representations of conservation laws of physics [8].

##### 2.1.1.1 Continuity equation

The continuity equation is based on the law of conservation of mass in a control volume, i.e. the rate of increase of mass in a fluid element must be equal to the net rate of flow of mass into the fluid element. It can be written as,

$$\frac{\partial \rho}{\partial t} + \text{div}(\rho \mathbf{u}) = 0 \quad (2.1)$$

where,  $\rho$  is the density of the fluid,  $\mathbf{u}$  is the velocity vector in the three dimensions and  $t$  is the time.

For an incompressible flow, the density is a constant therefore the equation becomes

$$\text{div}(\mathbf{u}) = 0 \quad (2.2)$$

##### 2.1.1.2 Momentum equation

The momentum equation is based on Newton's second law of motion which states the rate of change of momentum in a fluid particle is equal to the sum of forces acting

on the fluid particle. In CFD, this is applied to a fluid volume. The momentum equation is written as follows:

$$x\text{-momentum} \quad \frac{\partial(\rho u)}{\partial t} + \text{div}(\rho u \mathbf{u}) = -\frac{\partial p}{\partial x} + \text{div}(\mu \text{grad } u) + S_{Mx} \quad (2.3)$$

$$y\text{-momentum} \quad \frac{\partial(\rho v)}{\partial t} + \text{div}(\rho v \mathbf{u}) = -\frac{\partial p}{\partial y} + \text{div}(\mu \text{grad } v) + S_{My} \quad (2.4)$$

$$z\text{-momentum} \quad \frac{\partial(\rho w)}{\partial t} + \text{div}(\rho w \mathbf{u}) = -\frac{\partial p}{\partial z} + \text{div}(\mu \text{grad } w) + S_{Mz} \quad (2.5)$$

In this equation,  $u$ ,  $v$  and  $w$  represent the velocity in the  $x$ ,  $y$  and  $z$  directions respectively,  $p$  represents the pressure and  $\mu$  is the dynamic viscosity.  $S_m$  represents the sources term which would include the body forces in all three directions. A common body force is the force due to gravity.

### 2.1.1.3 Energy equation

The energy equation is based on the first law of thermodynamics which states that the rate of change of energy in a fluid particle equals the sum of the net rate of heat addition to the fluid particle and the net rate of work done on the particle. In CFD, the equation is applied to a control volume instead of a fluid particle. The energy equation is written as,

$$\frac{\partial(\rho i)}{\partial t} + \text{div}(\rho i \mathbf{u}) = -p \text{div } \mathbf{u} + \text{div}(k \text{grad } T) + \Phi + S_i \quad (2.6)$$

In this equation,  $i$  represents the internal energy in the fluid volume and  $\mathbf{u}$  is the velocity vector in the three dimensions namely  $x$ ,  $y$  and  $z$ .  $k$  is the thermal conductivity of the fluid medium and  $T$  is the temperature of the fluid node.  $\Phi$  is the dissipation function that accounts for the effects due to the viscous stresses and  $S_i$  is the source term from the internal energy equation.

## 2.1.2 Turbulence modelling

Most of the fluid flow in real applications are turbulent in nature. Turbulence refers to the chaotic and irregular characteristics in fluid flow. Turbulent flows are in general characterized by the swirling of eddies and fluctuations in flow properties like velocity and pressure. Some of the characteristics of turbulent flows are; they occur at high Reynolds numbers, they are always three-dimensional and they are highly diffusive in nature.

### 2.1.2.1 The $k - \epsilon$ turbulence model

In order to capture the effect of turbulence in a flow, turbulence models are used. One such model is the  $k - \epsilon$  turbulence model, where  $k$  is the turbulent kinetic energy and  $\epsilon$  is the turbulent dissipation rate. The  $k - \epsilon$  is one of the Reynolds-Averaged-Navier-Stokes models in which the flow variables are divided into mean and fluctuating quantities. The mean flow properties are solved using the RANS

equations, whereas the fluctuations are accounted for by solving additional transport equations. The  $k - \epsilon$  turbulence model is a two-equation model in which the transport equations are solved for turbulent kinetic energy and turbulent dissipation rate which is used for calculating the turbulent length scale and turbulent viscosity apart from the general governing equations [3].

The turbulent length scale is given by,

$$\ell = \frac{k^{3/2}}{\epsilon} \quad (2.7)$$

And the turbulent viscosity is given by,

$$\nu_t = c_\mu k^{1/2} \ell = c_\mu \frac{k^2}{\epsilon} \quad (2.8)$$

in which  $c_\mu$  is an unknown constant.

## 2.2 Heat Transfer

Heat transfer is the flow of heat due to differences in temperature between points and the subsequent distribution and changes in the same. It concerns the exchange of mass, momentum and energy in the form of conduction, convection, and radiation. Two objects initially at different temperatures, when kept in contact, eventually reach equilibrium temperatures according to the zeroth law of thermodynamics[1]. The amount of heat transferred is proportional to the temperature difference between the two points which is given by:

$$Q = mC_p\Delta T \quad (2.9)$$

where  $Q$  is the amount of heat transferred,  $m$  is the mass of the substance,  $C_p$  is the specific heat capacity of the substance and  $\Delta T$  is the change in temperature.

### 2.2.1 Conduction

Conduction is a phenomenon in which energy is transferred due to collisions between neighbouring atoms or molecules. It can take place in solids, liquids and gases. The basic form of the conduction equation is derived from the first law of thermodynamics and the equation given by:

$$\left( \frac{\partial}{\partial x} \left( K \frac{\partial T}{\partial x} \right) + \frac{\partial}{\partial y} \left( K \frac{\partial T}{\partial y} \right) + \frac{\partial}{\partial z} \left( K \frac{\partial T}{\partial z} \right) + E_{gen} \right) = \rho C_p \frac{\partial T}{\partial t} \quad (2.10)$$

where  $\frac{\partial^2 T}{\partial x^2}$ ,  $\frac{\partial^2 T}{\partial y^2}$ , and  $\frac{\partial^2 T}{\partial z^2}$  are the fluxes in the x, y, and z directions,  $E_{gen}$  is the heat generated internally,  $K$  is the thermal conductivity,  $\rho$  is the density,  $C_p$  is the specific heat capacity and  $\frac{\partial T}{\partial t}$  is the differential change in temperature over time. By simplifying this equation in one direction, we obtain Fourier's equation for heat

conduction which is given by the formula:

$$Q = -KA \frac{\partial T}{\partial x} \quad (2.11)$$

Where  $Q$  is the heat flux,  $K$  is the thermal conductivity,  $A$  is the cross-sectional area normal to the direction of heat flow and  $\frac{\partial T}{\partial x}$  is the temperature gradient.

### 2.2.2 Convection

Convection is a form of heat transfer seen mostly in fluids. It is the transport of heat due to fluid movement. Depending on the fluid movement, convection can be classified into natural or forced convection. The former is caused by the effects of buoyancy due to changing temperature fields. This is influenced by gravity. The latter is caused due to external means like pumps, fans or other devices. Convection is governed by Newton's law of cooling which is given by the formula:

$$Q = hA(T_s - T_\infty) \quad (2.12)$$

where  $Q$  is the rate of heat transfer,  $h$  is the convective heat transfer coefficient,  $A$  is the surface area over which heat transfer occurs,  $T_s$  is the surface temperature, and  $T_\infty$  is the bulk fluid temperature.

### 2.2.3 Radiation

Radiation is a mode of heat transfer where it does not require a medium for its propagation. This is quite different from convection and conduction. Solids, liquids and gases emit radiation in the form of electromagnetic waves, the intensity of which depends on the temperature of the substance as well as the nature of its surface. This type of heat transfer can be described with respect to a black body. A black body is a hypothetical body that absorbs all the light that falls on it. The radiation energy from the black body is given by Stephan Boltzmann's law which is given by the equation:

$$Q = \epsilon \sigma AT^4 \quad (2.13)$$

where  $Q$  is the rate of radiation heat transfer,  $\epsilon$  is the emissivity of the surface,  $\sigma$  is the Stefan-Boltzmann constant,  $A$  is the surface area of the object and  $T$  is the absolute temperature of the object.

### 2.2.4 Dimensionless numbers

Dimensionless numbers in heat transfer are used to obtain similitude between cases which can be different. The governing equations of fluid flow need to be in non-dimensional form for theoretical and computational reasons. There are mainly 4 dimensionless numbers used in heat transfer study

- Nusselt number
- Grashof Number
- Reynolds number
- Prandtl Number

#### 2.2.4.1 Nusselt Number

Nusselt number is defined as the ratio of convective to conductive heat transfer at any boundary. This includes both convection and conduction. Depending on the range of values, the flow can be classified as pure conduction, slug or flow dominated by convection. The formula is given by

$$\text{Nu} = \frac{\text{convective heat transfer}}{\text{conductive heat transfer}} = \frac{hL}{K}$$

where Nu is the Nusselt number,  $h$  is the convective heat transfer coefficient,  $L$  is the characteristic length and  $K$  is the thermal conductivity.

#### 2.2.4.2 Grashof Number

The Grashof number is a dimensionless number that relates the buoyancy and viscous forces together acting in a fluid. When the temperature of a fluid increases, the density decreases and hot air rises up. The force that opposes this motion is the viscous force. There are various formulations for Grashof number for different bodies. One such formulation is:

$$\text{Gr} = \frac{g\beta(T_s - T_\infty)L^3}{\nu^2}$$

where Gr is the Grashof number,  $g$  is the acceleration due to gravity,  $\beta$  is the thermal expansion coefficient,  $T_s$  is the surface temperature,  $T_\infty$  is the surrounding fluid temperature,  $L$  is the characteristic length and  $\nu$  is the kinematic viscosity. The above formula is for vertical flat plates.

#### 2.2.4.3 Prandtl Number

The ratio between momentum diffusivity and thermal diffusivity is given by the dimensionless Prandtl number. This is given by the formula

$$\text{Pr} = \frac{\mu \cdot c_p}{k}$$

where Pr is the Prandtl number,  $\mu$  is the dynamic viscosity,  $c_p$  is the specific heat at constant pressure and  $\alpha$  is the thermal diffusivity.

The physical significance of this number is that if values are much smaller than 1, thermal diffusivity dominates and in vice versa, momentum diffusivity dominates. In problems relating to heat transfer, the relative thickness of momentum and thermal boundary layers are controlled by the Prandtl number.

### 2.2.4.4 Reynolds Number

Reynolds number is the ratio between inertial forces to viscous forces. At low Reynolds numbers, the flow tends to be laminar and is dominated by viscous forces and at higher Reynolds numbers, the flow is turbulent and dominated by inertial forces. The formula for this number is given by

$$\text{Re} = \frac{\rho \cdot V \cdot L}{\mu}$$

where  $\text{Re}$  is the Reynolds number,  $\rho$  is the fluid density,  $V$  is the characteristic velocity,  $L$  is the characteristic length and  $\mu$  is the dynamic viscosity.

Reynolds number have a wide range of applications in thermal simulations. In forced convection simulations, it helps to select appropriate correlations for heat transfer calculations and pressure drop. In the case of natural convection where heat transfer is by buoyancy effects, Reynolds number helps to determine the boundary between the laminar and turbulent natural convection.

## 2.3 Co-Simulation

Co-simulation is the process in which two or more simulation software that are capable of operating independently are simulated together as one system. During a co-simulation, these stand-alone simulators are brought under a common platform where they are coupled together, such that the results from both simulators have an effect on the output of the system.

There are various reasons why co-simulation is used. One of the main reasons is to capture the physics of the system more effectively. This process uses the strengths of different software and couples them together so that, in a multi-physics system the model would be more accurate than it would have been in a stand-alone simulator. Since most of the simulation tools are catered towards specific physics, they would have been developed in such a way that they can give faster results when that specific physics is modelled and simulated. Therefore, using two different tools for multi-physics capabilities will reduce the overall computational time.

Communication and synchronization are two main aspects of any co-simulation. Synchronization of the two simulators is usually taken care of by the co-simulation interface provided the files from the different simulation tools are compatible. Communication is the process in which the two simulation tools interact with each other to exchange data at discrete intervals which can be specified by the user under certain modelling terms pertaining to that software.

# 3

## Methods

The thesis aims to develop and study a thermal model that can capture the cabin temperature accurately at different positions inside the cabin. The modelling is done through a two stage process. The first stage is developing a cabin model by co-simulation with GT-Suite and TAItherm which is referred to as GT-Flow Solution. The second stage is using CFD maps from a 3D CFD software into the co-simulation referred here as CFD flow field mapping. Both methods have been tried out and their accuracy has been evaluated by comparing them with test data. Both these methodologies have been discussed in detail in this chapter. In order to protect the sensitivity of the information about the model used for the thesis, the images illustrating the model have been replaced with a different cabin model of another car.

### 3.1 GT-Flow Solution

The GT-Flow Solution is the modelling approach for the thermal cabin model that involves co-simulating with GT-Suite and TAItherm without involving a 3D CFD software. The model developed with this method is rather a low-fidelity model that requires manual calibration to match the results from test data. In this case, the model is calibrated with the Heat transfer Coefficient Multiplier (HTCM), which scales the heat transfer coefficient between the cabin wall structure model in TAItherm and the fluid domain in GT-Suite. To understand this modelling approach, it is essential to know the working of co-simulation between GT-Suite and TAItherm which is discussed in detail in the following sections.

#### 3.1.1 Co-Simulation with GT-Suite and TAItherm

This co-simulation process involves GT-Suite solving the fluid domain in the cabin and TAItherm solving the wall temperatures of the cabin. The wall temperatures that are solved in TAItherm are used as the boundary condition for the fluid domain. The co-simulation process tries to emulate the heat transfer between the fluid domain in the cabin and the cabin wall structures by solving them separately in different software. The discretization of the geometries is done differently in GT-Suite and TAItherm as they solve for different quantities

In GT-Suite, the domain is divided into discrete sub-volumes or flow cubes which are connected along their faces. The fluid governing equations, i.e. continuity and

momentum equations are solved within the flow cubes in order to simulate the fluid flow in the cabin geometry. TAItherm uses a mesh that is imported with the geometry by a pre-processing software. Since TAItherm is used for getting the wall temperatures of the cabin, it solves the energy equation on the solid structures of the cabin geometry. It tries to capture the heat transfer between the cabin walls and the atmosphere and the heat transfer within the cabin structure through conduction, convection and radiation.

Before running the co-simulation, it is essential that the meshes from the two models are mapped on each other and for a communication interval to be set. This is discussed more in the next sections. During co-simulation, GT-Suite solves the fluid domain in the cabin and communicates the fluid temperatures ( $T_{Fluid}$ ) and Heat Transfer Coefficients (HTC) to TAItherm. Simultaneously, TAItherm solves the energy equations on the cabin structure and communicates the wall temperatures ( $T_{Wall}$ ) to GT-Suite as depicted in Figure 3.1.

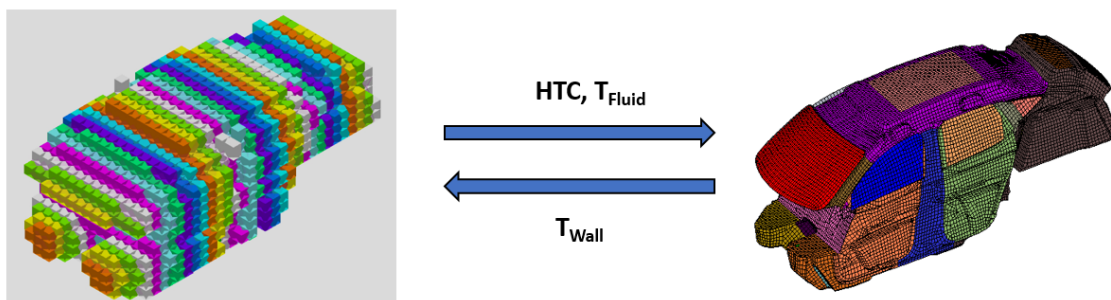


**Figure 3.1:** Representation of data exchange between GT-Suite and TAItherm models

#### 3.1.2 Mesh Mapping

In order for the models in GT-Suite and TAItherm to exchange information, it is essential that the meshes from the two models are mapped on each other correctly. The meshing is done differently in both the models as discussed in the previous section. The mesh mapping is done by the nearest cell approach, i.e. the mesh from one model maps itself to the nearest mesh element of the other model. Figure 3.2a shows the mesh from a door component in the TAItherm model being mapped onto the corresponding flow cubes in the GT-Suite model. Since the mesh in TAItherm is finer than the GT mesh, multiple elements from the TAItherm mesh will be mapped to a single flow cube as depicted in Figure 3.2b. A flow cube can only store a single value of a variable in its node, therefore the wall temperature stored in the TAItherm mesh elements within a flow cube is averaged and communicated with the flow cube. On the contrary, the fluid temperature ( $T_{Fluid}$ ) and Heat Transfer Coefficient (HTC) stored in a flow volume are exchanged with all the TAItherm mesh elements that are mapped on that particular flow cube in the GT model [2].

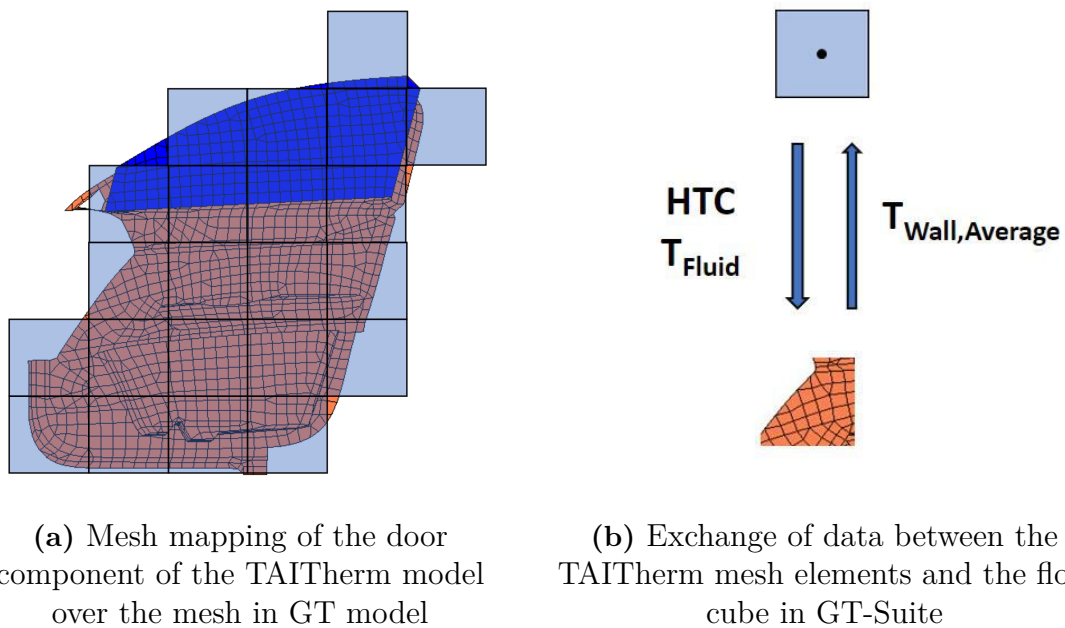


**Figure 3.2:** Representation of mesh mapping between GT-Suite and TAITherm

### 3.1.3 Communication interval

An important factor in the co-simulation process is the interval at which the data is exchanged between the two models which can be specified by the user as the communication interval. It is essential to set an appropriate communication interval, as too large an interval can cause instability in the solver during the run. On the other hand, too small of a communication interval would take up a lot of time for computation. Figure 3.3 is a schematic of how the data is exchanged between the models for a simulation time of 20 seconds. In this example illustrated in figure 3.3 the time step size in the GT model is set to 1 second and the time step size in TAITherm solver is set to 5 seconds. The communication interval is also set to 5 seconds. During co-simulation, the GT model solves the fluid domain every 1 second, whereas the TAITherm model solves every 5 seconds. At the 5-second interval, the data is exchanged between the models and the simulation proceeds forward. The process is repeated till the end of the run.

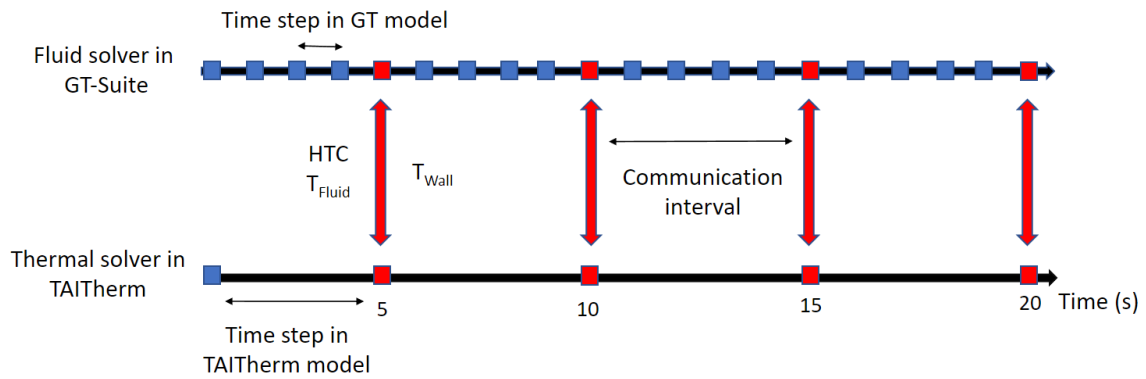


**Figure 3.3:** Time steps and communication intervals used in the co-simulation model

### 3.1.4 Work Process in GT-Flow Solution

The general workflow for the GT-Flow Solution is depicted in Figure 3.4. The 3D geometry of the car cabin is imported into ANSA for pre-processing and meshing purposes. The meshed geometry is imported as a Nastran file into TAItherm, where the geometry is modelled to replicate the wall structures of the cabin. The mesh file from ANSA is also imported into COOL3D - a 3D pre-processing tool in GT-Suite for defining the fluid domain. The discretized fluid domain is imported into the GT-ISE system simulation setup as a sub-assembly file. The TAItherm model is also imported into the GT-ISE setup which is prepared for co-simulation by defining the relevant conditions required by the setup. This is discussed further in the following sections [7].

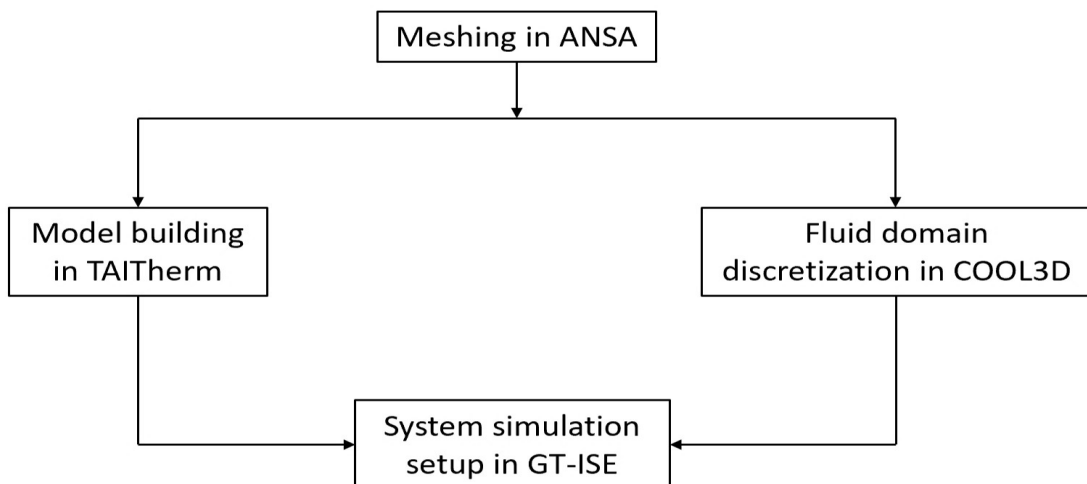


**Figure 3.4:** Flow chart of the work process for GT-Flow Solution

#### 3.1.4.1 Pre-processing and Meshing in ANSA

The first step in building the co-simulation model is preparing the CAD geometry used for the simulations. ANSA is a pre-processing tool that can be used for cleaning the geometry and meshing as per requirement. The CAD model in ANSA is the cabin geometry, i.e. the volume of the space occupied by the air inside the cabin. This model is used in both COOL3D and TAITherm. The primary step in cleaning the CAD model is checking the model for leaks. In order for the COOL3D to process the geometry as a fluid domain, it is essential an air-tight leak-free mesh model is imported to it. Therefore, the model is sealed in places of leaks in ANSA before meshing. Once the model is cleaned, the meshing was done. The meshing needs to be done as required by the TAITherm model, as the TAITherm model uses the mesh provided to it by ANSA. For thermal solvers in solid structures, it was deemed that a quadrilateral mesh best serves the purpose. Hence, a quadrilateral mesh is made in ANSA. Figure 3.5 shows the cleaned and meshed geometry in ANSA that was further used in TAITherm and COOL3D models

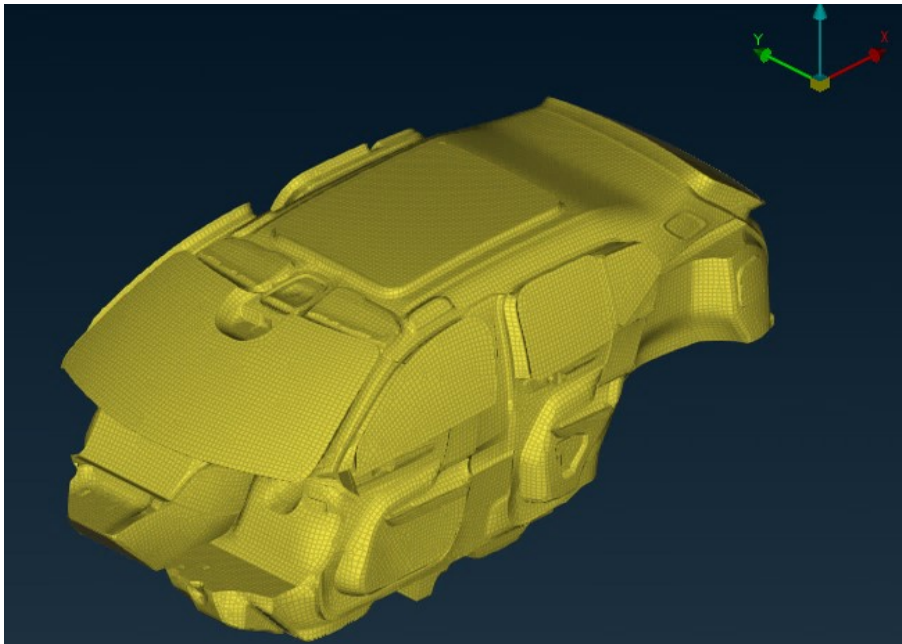


**Figure 3.5:** Meshed model in ANSA

#### 3.1.4.2 Model Building in COOL 3D

COOL3D is a pre-processing tool available within GT-Suite which is used for the discretization of the fluid domain in order to solve for the flow inside the cabin. To discretize the cabin, the meshed cabin volume is imported to COOL3D and converted into a flow space. The parts inside the cabin which includes the seats are converted into flow blockages. Once all the flow blockages are created, the rectangular vent openings are added to the cabin as per the requirements. Inlet and outlet vents are defined at various positions of the cabin with specified dimensions and normal indicating the flow direction was specified as well. In order to effectively capture the temperature inside the cabin domain, multiple temperature sensors are added

at various positions, that includes head, chest and feet for the two seats in the front and rear.

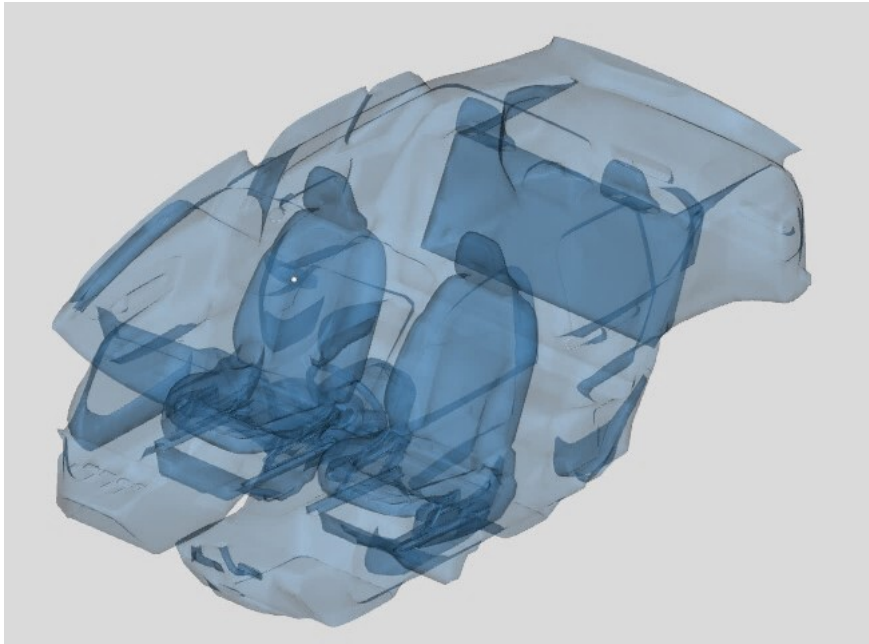


**Figure 3.6:** Flow space defined in COOL3D

The discretization of the fluid domain was done by dividing the domain into sub-volumes or flow cubes with prescribed dimensions. For this study, flow cubes of size 100x100x100 mm were used. Figure 3.7 shows the discretized fluid domain containing flow cubes of size 100x100x100 mm. The discretized model is exported as a sub-assembly file into the GT-ISE system simulation setup.

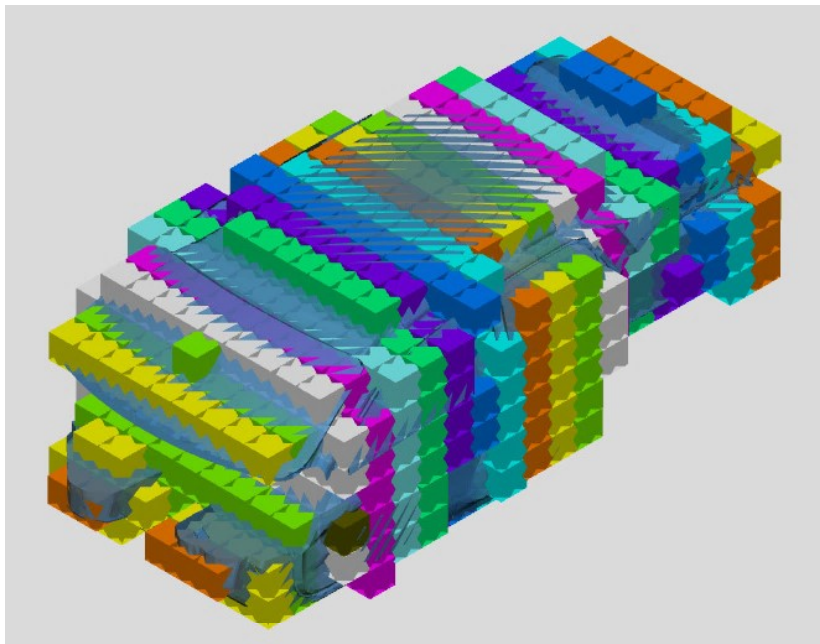


**Figure 3.7:** Discretized flow space in COOL3D

### 3.1.4.3 TAItherm model

To model the wall temperatures, the thermal properties and the materials of different parts of the cabin are assigned in the TAItherm software. The initial model was a full-sized design of the vehicle with a lot of intricate parts and components. The time required to simulate this model was very high due to a large number of mesh elements. Because of this, the full-size vehicle model was converted to a multi-layered cabin model with calculated properties. This reduced the overall mesh elements and gave a good reduction in simulation time also with good control over the material properties. The properties of all the parts of the cabin were calculated by taking the area-weighted average of density, conductivity and specific heat along a particular layer. A simple heat-up simulation with TAItherm was conducted in both the full model and the multi-layered model. The results from them showed that both models behaved similarly in terms of representing the thermal masses in the cabin. Hence the multi-layered cabin model was chosen for the co-simulation.

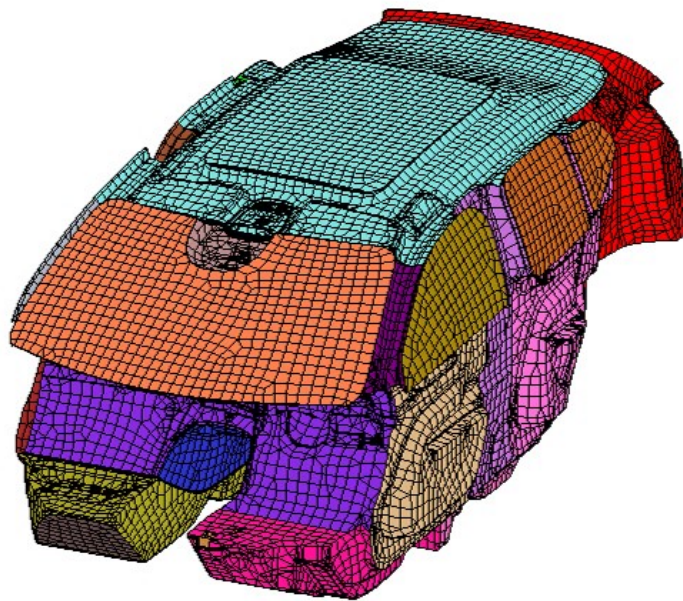


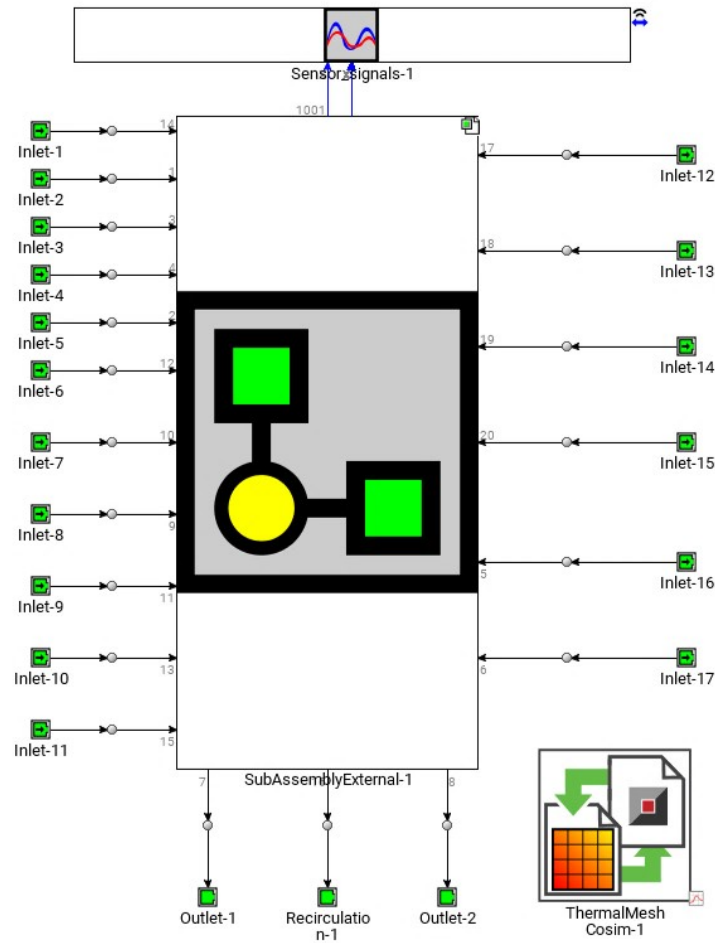
**Figure 3.8:** TAItherm model

The outer layer of the thermal model in TAItherm was assigned convective boundary conditions by specifying the wind velocity and ambient temperature.

Based on those conditions and the dimensions of the parts exposed to the ambient, TAItherm calculates the HTC and models the heat transfer appropriately. The inner layer of the model is set to the co-simulation conditions, i.e, they receive the HTCs and  $T_{Fluid}$  values from the fluid domain model in GT-Suite.

### 3.1.4.4 System simulation setup in GT-ISE

GT-ISE is the interface in GT-Suite that is used to develop system-level simulation models. In this case, it is used for building the thermal model of the cabin which can be integrated with a larger system setup that might comprise the entire components of the climate system in a car. This climate system may include fans, compressors, heaters, chillers, air filters and other components in the HVAC system. However, this thesis only focuses on developing a cabin thermal model with system simulations.



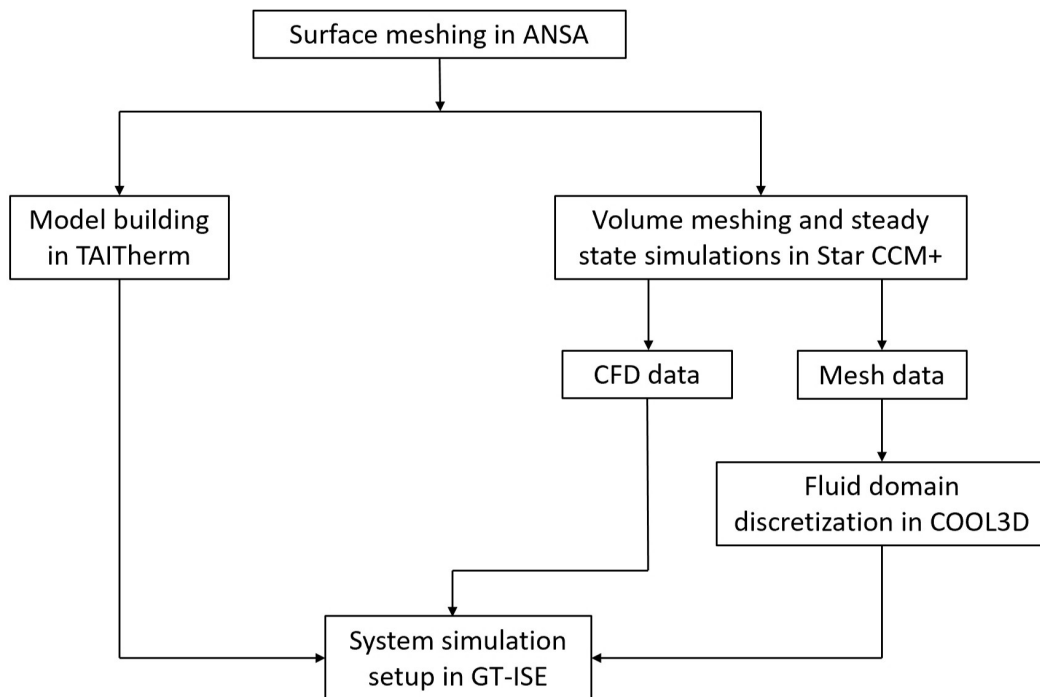
**Figure 3.9:** System simulation setup in GT-ISE

Figure 3.9 is a representation of the system simulation setup that was made in GT-ISE. The sub-assembly file imported from COOL3D is placed in the SubAssemblyExternal template. The inlet vents in the cabin are modelled as mass flow inlets which are connected to the sub-assembly file. The outlets are modelled as pressure outlets. A re-circulation vent could be used in the model if the re-circulation is enabled in the HVAC system. The sensors that were placed in the cabin model in COOL3D are connected to the Sensorsignals-1 template, such that the temperature at those sensor positions is recorded during the simulation. The co-simulation parameters such as the TAItherm file, communication interval and Heat Transfer

Coefficient Multiplier (HTCM) are defined in the ThermalMeshCosim-1 template.

## 3.2 CFD flow field mapping

In order to avoid the need for calibration and to get a more accurate high-fidelity model, the CFD flow field mapping method needs to be employed. This method is an extension of the GT-Flow Solution where a 3D CFD software is used to solve the flow field inside the cabin as a steady-state solution. This solution data obtained from CFD results is mapped onto the co-simulation model which gives a more accurate flow distribution as it captures the velocity profiles, pressure gradients and turbulence precisely. Once these data are fed into the co-simulation interface the Heat Transfer Coefficients (HTCs) can be predicted more accurately.



**Figure 3.10:** Process flow when CFD flow field mapping is used

Figure 3.10 illustrates the process flow for the cabin model development when CFD flow field mapping is used. The surface mesh file from ANSA is exported to Star CCM+, where the volume is meshed, and the inlets and outlets are defined. The model is set up for the steady simulation by specifying the boundary condition and choosing the appropriate physics models. Multiple steady state simulations were done, one for each fan speed which would change the inlet conditions in the cabin. The geometry file from Star CCM+ is exported to COOL 3D where the domain is discretized into flow cubes for the co-simulation. The fluid flow data in the fluid domain in Star CCM+ is exported to the GT-ISE system simulation setup, so that

the steady state solutions can be mapped on to the co-simulation interface.

#### 3.2.1 Set up in Star CCM+

Once the surface mesh file from ANSA is imported to Star CCM+, the cabin model has to be meshed appropriately. This involves refining the mesh in places with high temperature and velocity gradients, which are region close to the inlets and defining prism layers near the wall, so that the near-wall effects can be captured well.

Figure 3.11 and 3.12 show the mesh that was used in Star CCM+ for running the steady-state simulations. The inlets through which the air enters the cabin are only present at the foot region in the cabin. Hence those regions are refined to a finer mesh to capture the high velocity and temperature gradients that could occur at the foot region. During the testing, it was found that some amount of air enters through the vents at the door, so some refinement was needed near the rear doors. It can also be seen that prism layers were defined at walls enclosing the fluid domain.

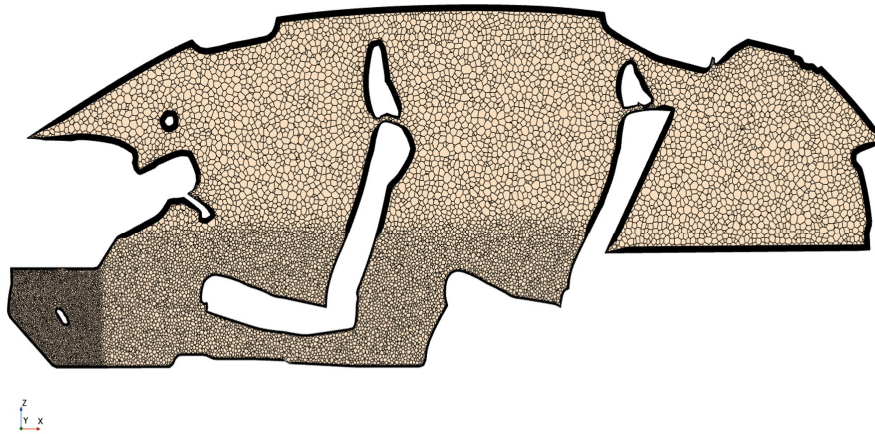


**Figure 3.11:** Cross sectional side view of the meshed geometry

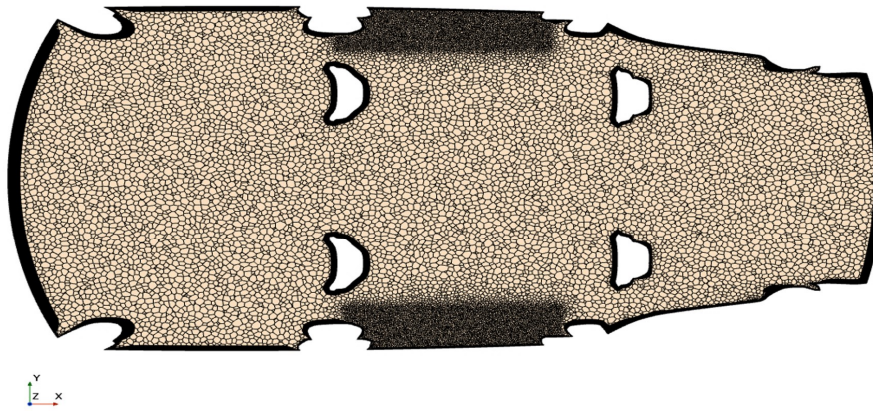


**Figure 3.12:** Cross sectional top view of the meshed geometry

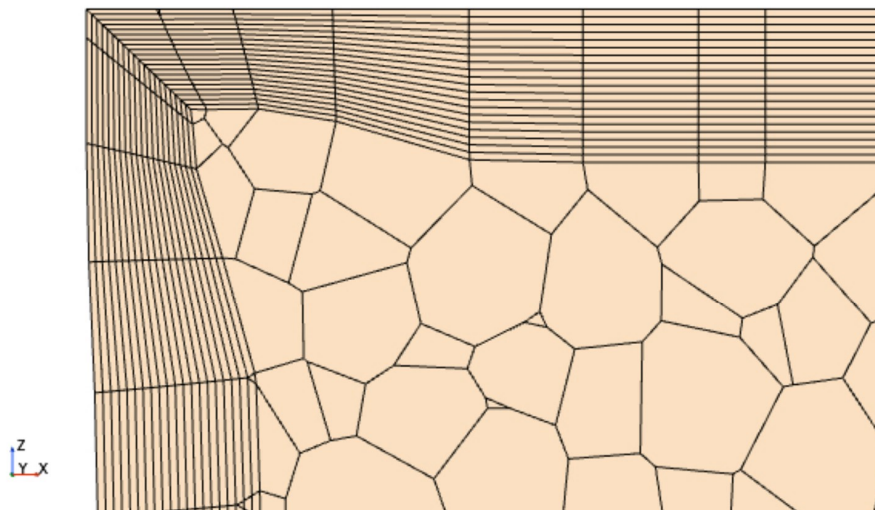


**Figure 3.13:** Prism layers in the mesh

Figure 3.13 shows the zoomed view near the fluid domain walls located at the foot region. The prism layers used in the mesh can be seen in this figure. It is essential to have prism layers in any mesh used for fluid flow simulations, as they help to capture the near-wall effects. The prism layer helps to capture the boundary layer growth that occurs on the wall surface of the fluid domain. Unlike bulk fluid motion away from the wall, the fluid flow near the walls is influenced by the no-slip condition. These prism layers help to emulate the flow near the walls.

In order to obtain accurate results, it is imperative to set up the CFD solver with the right physics. Table 3.1 below gives different physics models that were chosen. The fluid material was air with corresponding mass flow rates at the inlets and pressure conditions at the outlet. Coupled flow was used for this simulation as there is a strong, interaction between airflow and temperature gradients. So coupled flow gives a stronger representation of the interactions by simultaneously solving the equations together. The equation of state describes how the properties inside the cabin change due to changes in pressure, temperature, volume, etc. The selected model was Real Gas with Equilibrium air. The turbulence model chosen was the K-Epsilon model, as it is a simpler model and solves comparatively faster than other turbulence models. After meshing the geometry and setting the right physics, the inlet conditions were given based the chosen fan speed; by specifying the mass flow rate and temperature of the air entering the cabin which was measured in the experiments. The simulations were run till they reached a steady state.

<b>Physics parameter</b>	<b>Chosen model</b>
Space	Three-dimensional
Material	Gas
Time	Steady
Flow	Coupled Flow
Equation of State	Real Gas (Equilibrium Air)
Energy	Coupled
Viscous Regime	Turbulent
Turbulence Model	K-Epsilon Turbulence Realizable k-epsilon Two layer Two layer all Y+ wall distance

**Table 3.1:** Physics models chosen for the steady state simulations

#### 3.2.2 Discretization in COOL3D

The mesh data from the Star CCM+ model is exported into COOL3D as a geometry file. When the model is discretized by this method, the inlet and outlet vents defined in Star CCM+ is taken as the inlets and outlets in the COOL3D model. The fluid domain defined in the Star CCM+ model is taken as flow space in COOL3D. The sensors are placed inside the cabin where the temperatures need to be measured.

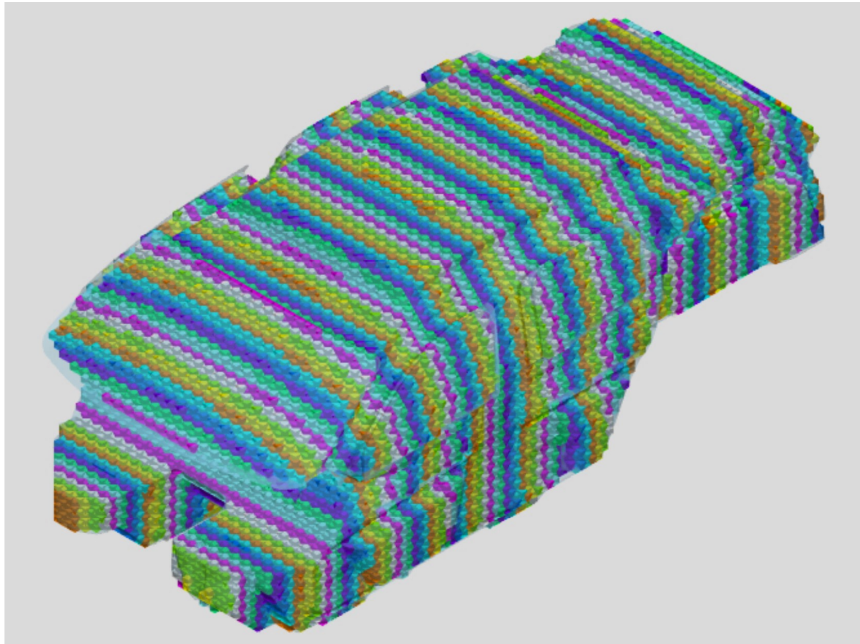


**Figure 3.14:** Discretized flow space in COOL3D using the mesh file from Star CCM+

Figure 3.14 shows the flow space that was discretized based on the mesh file imported from Star CCM+. It can be seen that the flow cubes are of size 30x30x30 mm which is much smaller than the flow cubes defined in the GT-Flow solution method which were 100x100x100 mm. Once the sensors are placed in the COOL3D model and the flow space is discretized, the model is exported to GT-ISE as a sub-assembly file along with certain flow parameter data that was exported from Star CCM+. The procedure following this is same as the one described for the GT-Flow Solution method.

### 3.3 Heat-up test setup

The model built using the two different methods needed to be validated using data from experiments. A heat-up test was performed in a climate wind tunnel. The model was built to simulate the test conditions such that the values from the test and model were comparable. The heat-up test involves placing the car in a cold ambient temperature and heating up the cabin to a comfortable temperature by HVAC systems.

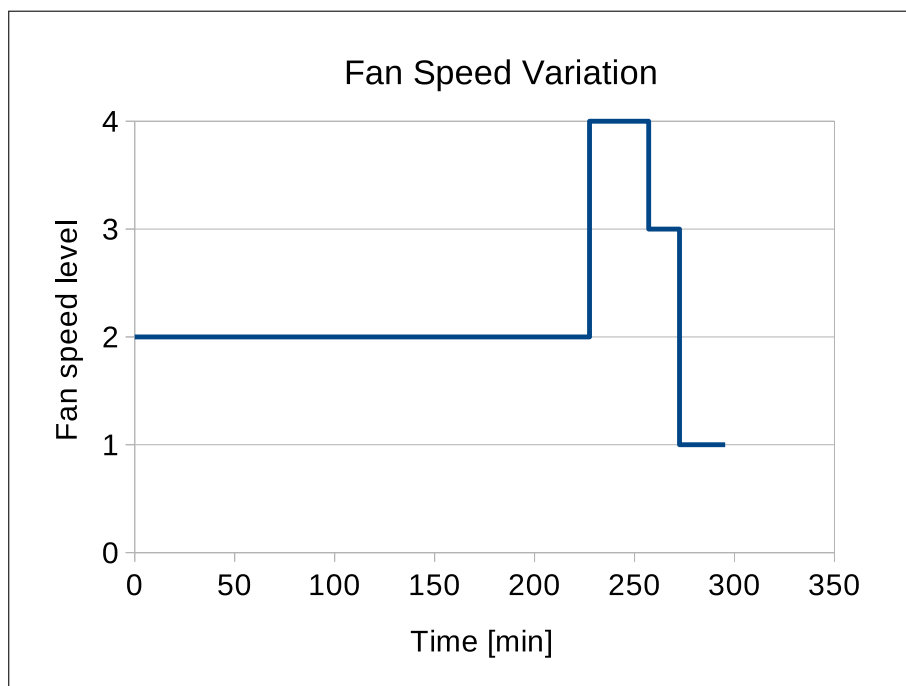
Ambient temperature	$-18^{\circ}C$
Wind speed	50 km/hr
Fan speeds in HVAC system	variable
Active vents from HVAC	Floor vents
Presence of Re-circulation	No
Total run time	295 mins

**Table 3.2:** Heat-up test parameters

The test parameters used in the heat-up testing in the wind tunnel is briefly explained in Table 3.2. The wind speed on the car standing still replicates the wind over the car moving at a certain speed in still air. The wind speed would greatly influence the convective heat transfer between the car body and the ambient. This makes the wind speed the most essential factor in a climate wind tunnel.

Before the test starts, it is necessary to get the cabin temperature down to the cold ambient temperature set in the wind tunnel. To ensure this, the car is left in the cold wind tunnel for a few hours until the cabin temperature is close to the cold ambient temperature. This process is called soaking of the car to the ambient conditions.

The test is done to study the transient temperature change in the cabin for a certain fan speed of the HVAC. The fan speed controls the flow rate of the hot air entering the cabin. Once the cabin temperature reaches a steady state, different fan speeds are set for smaller time intervals to observe the temperature behaviour.



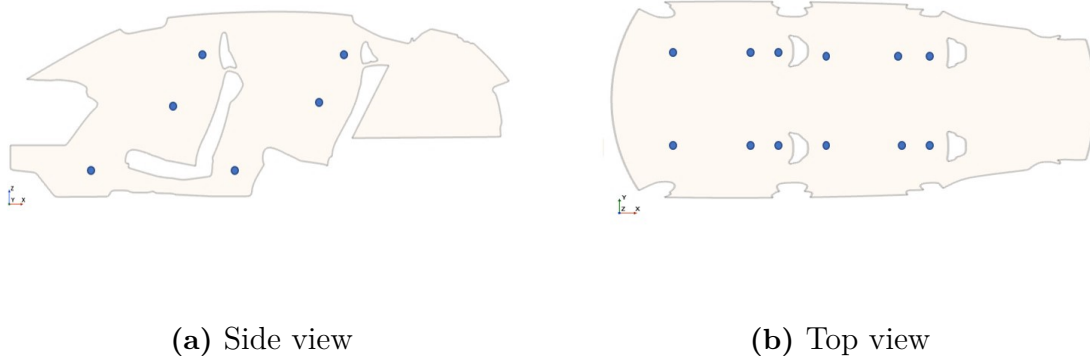
**Figure 3.15:** Different fan speeds

Figure 3.15 shows the different fan speeds that were used throughout the duration of the test. As seen in the figure, a fan speed level 2 was used for a major run time of the test in order to capture the transient temperature curves on the different sensors placed within the cabin. Once it reached a steady state, the fans speed was varied to level 4, level 3 and level 1 for the rest of the test to study the trend in the temperature curves for different inlet conditions.

To test the accuracy of the model with the experiments and to determine how much calibration would be required, the initial set of simulations were only done for the first fan speed, i.e. level 2. Once the model was deemed accurate enough, the simulation was extended to other fan speeds to check the robustness of the model developed.

### 3.4 Sensor positioning

In order to record the temperatures at different positions in the cabin, temperature sensors were placed at various positions inside the cabin during the heat up test experiment. To compare the temperature data from the experiment, sensors were placed at the same locations in the cabin model in COOL3D which was discussed in section 3.1.4.2.



**Figure 3.16:** Schematic of the cabin with sensor positions

As seen in figure 3.16, there are 12 zones inside the cabin, at which the temperatures were recorded. These 12 zones include the head sensors, chest sensors and foot sensors in all four seats in the cabin. These four seat positions are referred to as driver, passenger, rear left and rear right. Multiple sensors were placed in each zone so that the average of sensors temperature in each zone will give the temperature at that zone. This was done in the experiment as well as in the simulation model. The temperature recorded at each zone in the experiment and model were compared.



# 4

## Results and Discussion

The results of the thesis work mainly involve studying the transient temperature curves at different location inside the cabin model and comparing them with the experimental results. The results from both the methods, i.e. GT-Flow Solution that does not include mapping data from a 3D CFD software and the solution with the 3D CFD flow field mapping is discussed in detail in the following sections. To protect the sensitivity of the data in the plots, the data is normalized and illustrated in the figures.

### 4.1 TAITherm mesh study

The TAITherm model used in the co-simulation is one of the most essential attribute of the modelling process. The thermal masses inside the cabin and on the walls has to be captured properly in order to emulate the heat transfer between the fluid domain and the cabin accurately. These thermal masses are modelled in the TAITherm model. The mesh used in the TAITherm model has to fine enough to capture the heat transfer through the solid structures. The TAITherm model has a significant impact on the total computational time for the co-simulation. Therefore, it is also important to choose a mesh that gives accurate results and also takes lesser time for computation.

A mesh study with TAITherm model was done to ensure an appropriate mesh is chosen for the co-simulation. The simulation was set up by modelling the mesh file to replicate the thermal masses in the car cabin. The ambient conditions were similar to that of the experiment and the temperature of the air node placed inside the TAITherm model was studied. The air node was linked with a another air node with hot air condition and certain mass flow rate through an advection link. This was done to emulate the hot air entering the cabin during the test. The process was repeated for different meshes and the temperature curves was compared.

Mesh 1	15330 elements
Mesh 2	22886 elements
Mesh 3	37608 elements
Mesh 4	51578 elements

**Table 4.1:** Different meshes tested

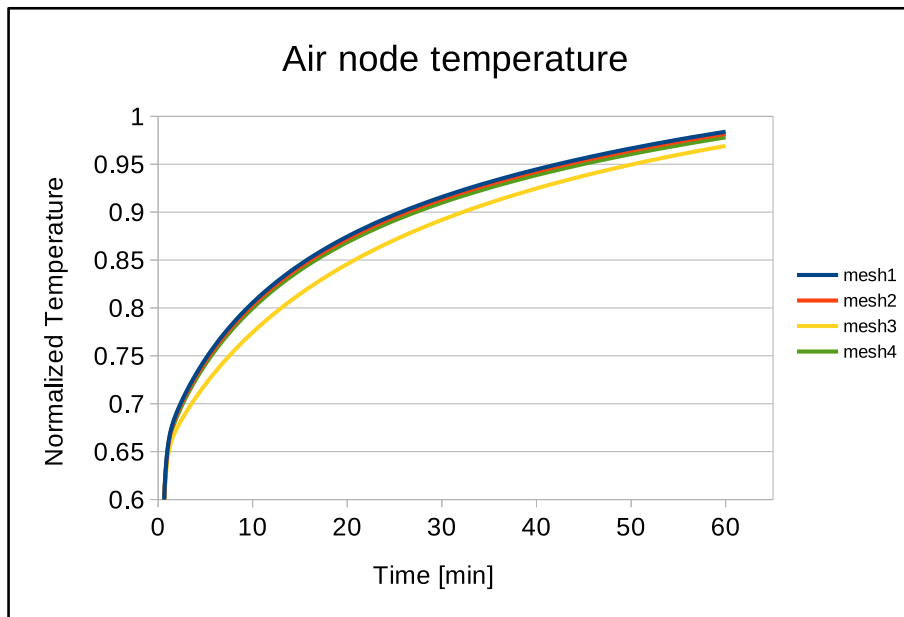


**Figure 4.1:** Temperature curves of the air node placed inside the cabin for different meshes

Figure 4.1 shows the heat-up curve for the air node placed in the TAITherm cabin model. The simulation was performed as standalone simulation in TAITherm to evaluate the fitness of the mesh. As seen in the figure, heat up curves have a similar trend for the different meshes. Based on the comparison of the temperature curves, it was determined that all the meshes behave similarly in terms of capturing the thermal masses and the heat transfer in the cabin structure. While it may seem that mesh 3 behaves slightly different from other meshes based on the curves in figure 4.1, the temperature difference between mesh 3 and other meshes was only around  $0.5\text{ }^{\circ}\text{C}$ . So, the mesh needed to be chosen based on a different parameter.

The duration of this simulation was 60 minutes with time step of 6 seconds, thereby a total of 600 time steps was computed by the software. Since the solution has to converge for each time step, it takes a certain number of iterations for every time step. Thus, the total number of iteration taken by the solver can be used as a reference to the time taken by the solver for computation, as the number of iterations was proportional to the simulation time in these simulations.

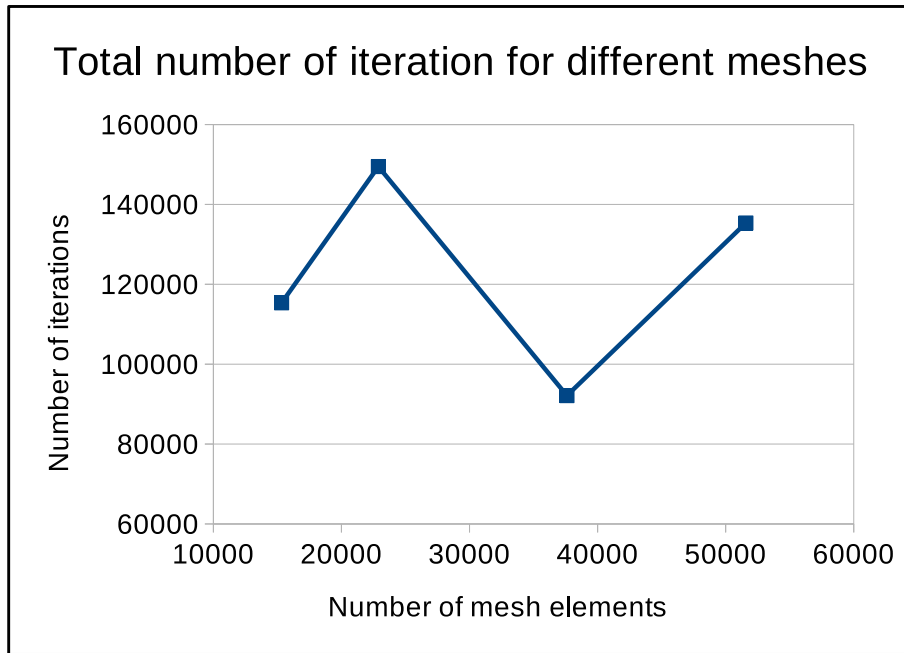


**Figure 4.2:** Number of iterations taken by the solver to compute for 600 time steps in different meshes

Figure 4.2 shows the number of iterations taken by the solver to solve for 600 time steps. The solver takes the least number of iterations to solve for 600 time steps while using mesh 3 with 37608 elements. This could be because the mesh 3 was a better mesh for the software to solve the energy equations within the structure. The solution was more stable with this mesh which led to lesser number of iterations for each time step resulting in lower computational time. Therefore, this mesh was chosen for the TAITherm model in the co-simulation setup.

## 4.2 GT-Flow Solution

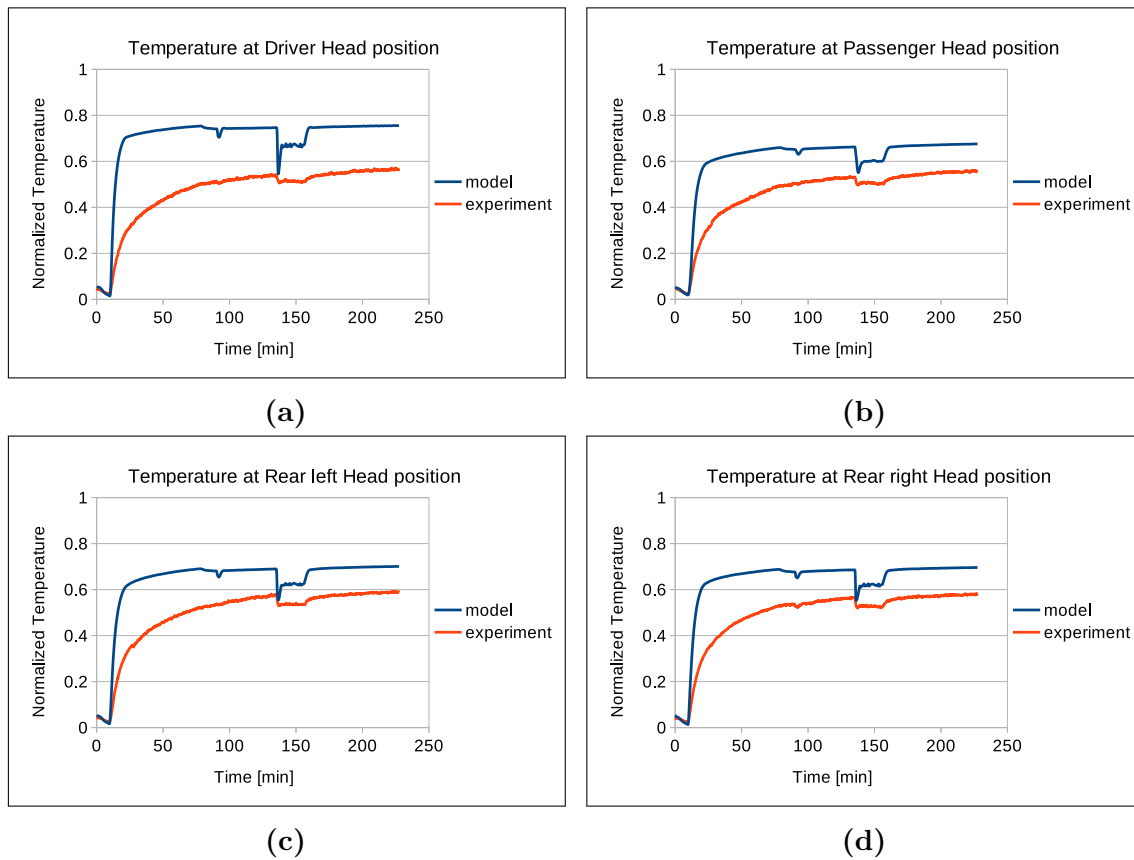
The solution with GT-Flow without using a 3D CFD map is a low-fidelity model. This model is relatively simpler in terms of complexity of the simulation setup, but the model requires a lot of manual calibration to fit the experimental data. To evaluate the required amount of calibration, the simulation was run without calibration initially. Based on the result of that simulation, the model was calibrated accordingly and the results were compared. This is discussed in detail in the following sections.

### 4.2.1 Results without calibration

For the initial simulation, the model was set up and run without calibration. The calibration parameter is the Heat Transfer Coefficient Multiplier which was set to the default value of 1. The simulation was run for the single fan speed and the results were compared with that of experiment. The temperature sensors were placed at 12

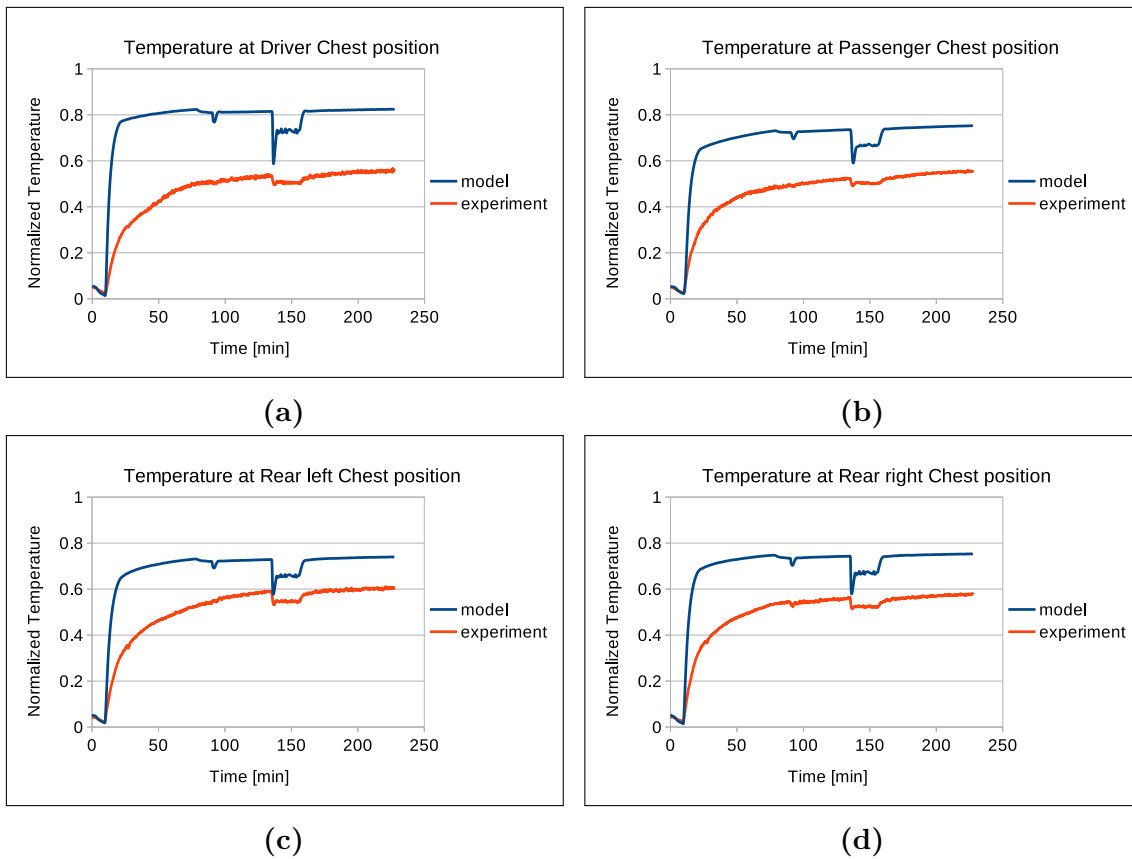
## 4. Results and Discussion

different locations at the cabin in both the experiment and the simulation, so that the corresponding temperatures can be compared.



**Figure 4.3:** Comparison of temperature curves from the experiment with the simulation model at the four head positions in the cabin which are (a) Driver (b) Passenger (c) Rear left seat (d) Rear right seat

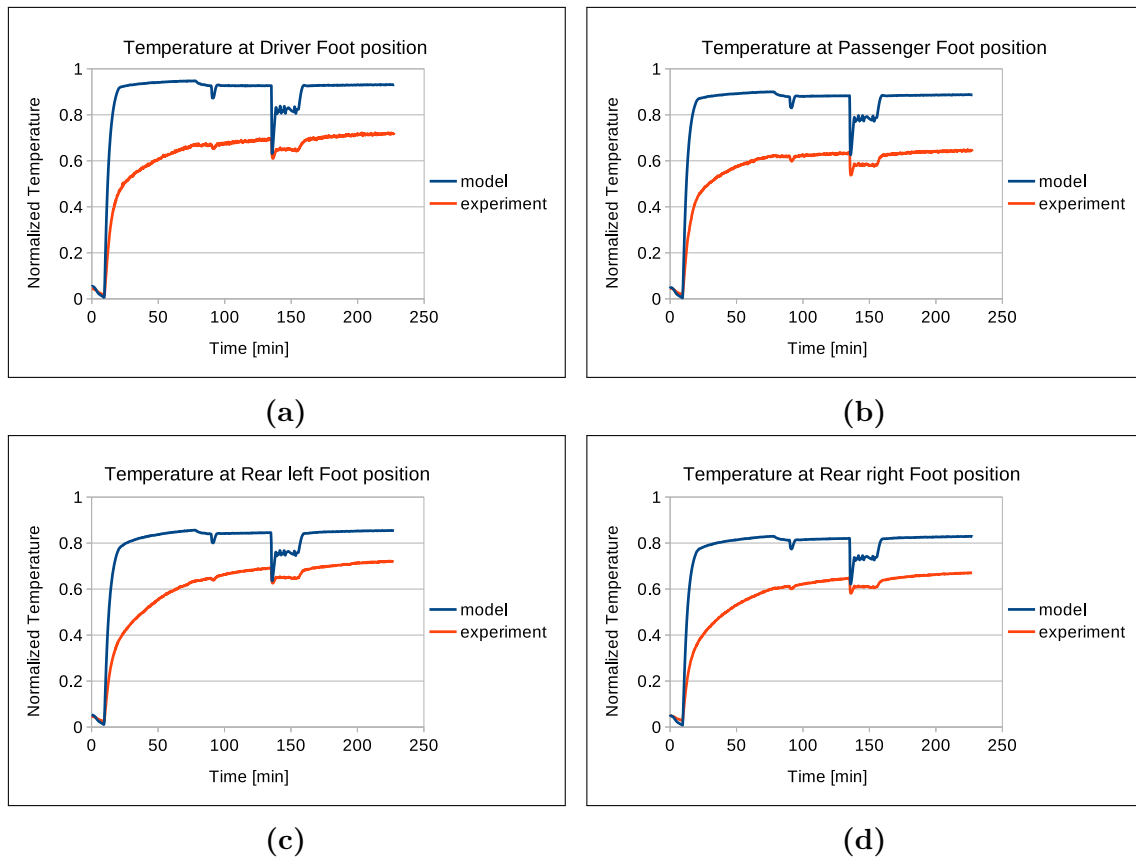
Figure 4.3 shows the temperatures curves that were measured by the sensors in the experiments as well as the simulation model. As it can be seen, there is a significant difference between the simulation and experiments. In order to get a better view of the results, the temperature plots for the other sensors were also plotted and studied.



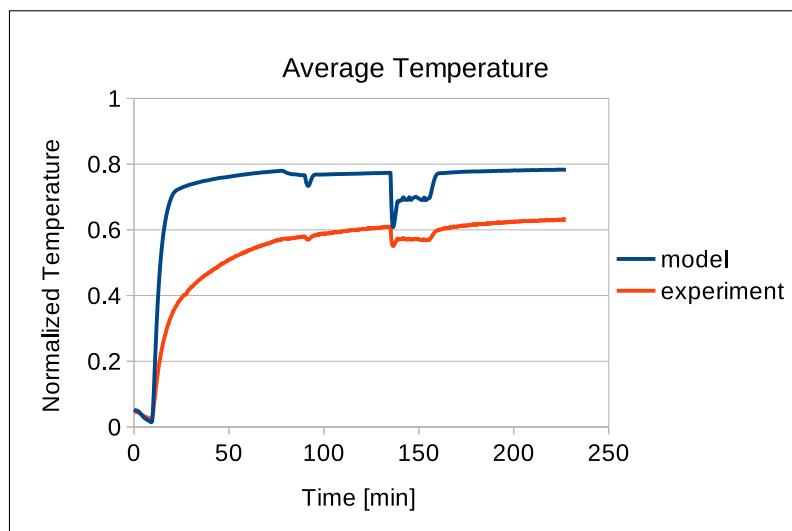
**Figure 4.4:** Comparison of temperature curves from the experiment with the simulation model at the four chest positions in the cabin which are (a) Driver (b) Passenger (c) Rear left seat (d) Rear right seat

Figure 4.4 and 4.5 shows the temperature curves at the various chest and foot positions respectively. It can be seen that at all the positions, the temperature recorded by the sensor in the model is much higher than the experiment. This is because the hot air inlets in the simulation have a direct impact on the temperature throughout the cabin model. This is the reason why the temperature in foot sensors have recorded a much higher temperature compared to the head and chest region in the simulation, since the hot air inlets are modelled at the foot vents. This results in high temperature gradients within the cabin in the simulation, which is not the case in experiments, where the temperature distribution is more uniform, with small differences between the head, chest and foot regions. The heat diffusion in the experiment is not captured well in the simulation leading to high temperature in the foot region compared to the head region.

## 4. Results and Discussion



**Figure 4.5:** Comparison of temperature curves from the experiment with the simulation model at the four foot positions in the cabin which are (a) Driver (b) Passenger (c) Rear left seat (d) Rear right seat



**Figure 4.6:** Average temperature recorded by all the 12 sensors placed in the cabin in experiments and simulation model

It can also be seen that the heat up curves are too steep, meaning the cabin gets heated up faster in the model than the experiment. The reason for this occurrence

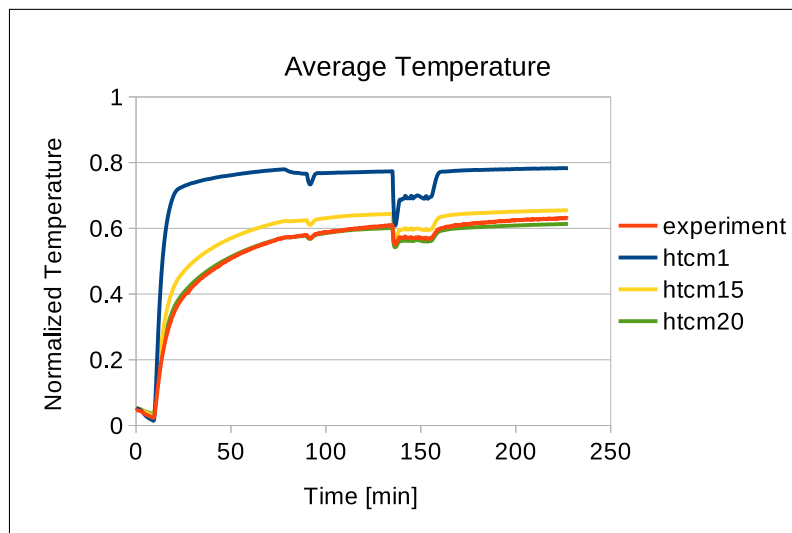
is that the heat transfer coefficients are not captured properly in the GT-Flow Solution and therefore need to be calibrated.

To calibrate the simulation data against the test data, one data set has to be chosen and kept as reference for calibration. In that case, if a particular sensor data is of interest, the model can be calibrated against that sensor data from the experiment. In this case, the average of all sensors is used as reference for calibration which is shown in figure 4.6, as the aim is to have a model with a good temperature distribution throughout the cabin.

#### 4.2.2 Results with calibration

In this methodology it was established that the model can be calibrated with the Heat Transfer Coefficient Multiplier (HTCM). The HTCM is a scaling factor for the heat transfer coefficient that affects the heat transfer between the cabin wall modelled in TAItherm and the fluid domain modelled in GT-Suite. When the model is not calibrated, the HTCM is set to the default value of 1, meaning the heat transfer coefficients are not scaled to any value but are rather taken as computed by the solver. This was discussed in detail in the previous section.

A HTCM of 15 and 20 was used in the model and the simulations was performed for the single fan speed similar to the simulations without calibration. The results from both the simulations were compared with the experimental data and with the results from the model with HTCM of 1, i.e. the simulation without calibration.



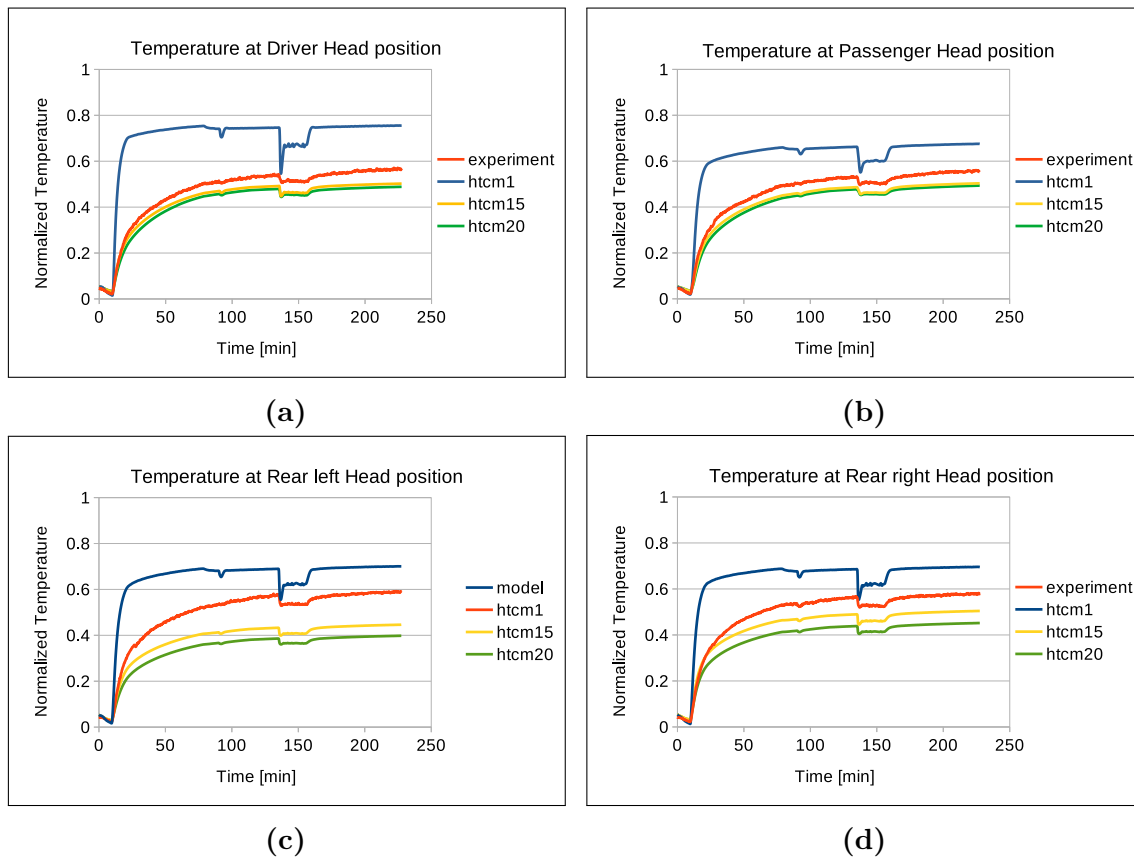
**Figure 4.7:** Average temperature recorded by all the 12 sensors placed in the cabin in experiments and simulation model

Figure 4.7 shows the temperature curves of the average temperature readings taken from all the sensors placed in the cabin in experiment as well as simulations. It can be seen when a HTCM of 15 and 20 are used to calibrate the model, the results from the simulation agree much better with the experiments than when HTCM of 1 is

## 4. Results and Discussion

used. Of the two calibration factors, the HTC<sub>M</sub> 20 is the closest to the experiment. This implies that the global heat transfer coefficient between the fluid domain and the wall structure needed to be scaled up by a factor of 20 in order to capture the heat transfer more accurately.

In order to see if this calibration is effectively at every region in the cabin, it is prudent to check the temperature curves at all the 12 sensor positions from which the average was calculated. It is essential for a thermal model to capture the temperature locally at each zone in the cabin and to check if the same calibration factor works at every sensor positions.



**Figure 4.8:** Comparison of temperature curves from the experiment with the simulation model at the four head positions in the cabin which are (a) Driver (b) Passenger (c) Rear left seat (d) Rear right seat

Figure 4.8, 4.9 and 4.10 depicts the temperature recorded by the head sensors, chest sensors and foot sensors respectively for the experiments and simulations. It can be seen how calibrating the model with HTC<sub>M</sub> of 15 and 20 affects the temperatures at the different zones in the cabin. Although for some regions like the driver head, passenger head and rear right chest position the calibrated simulation agrees quite well with experiments, for other regions there is a significant difference in temperature curves from the experiment and simulation even when the model is calibrated with a HTC<sub>M</sub> of 20.

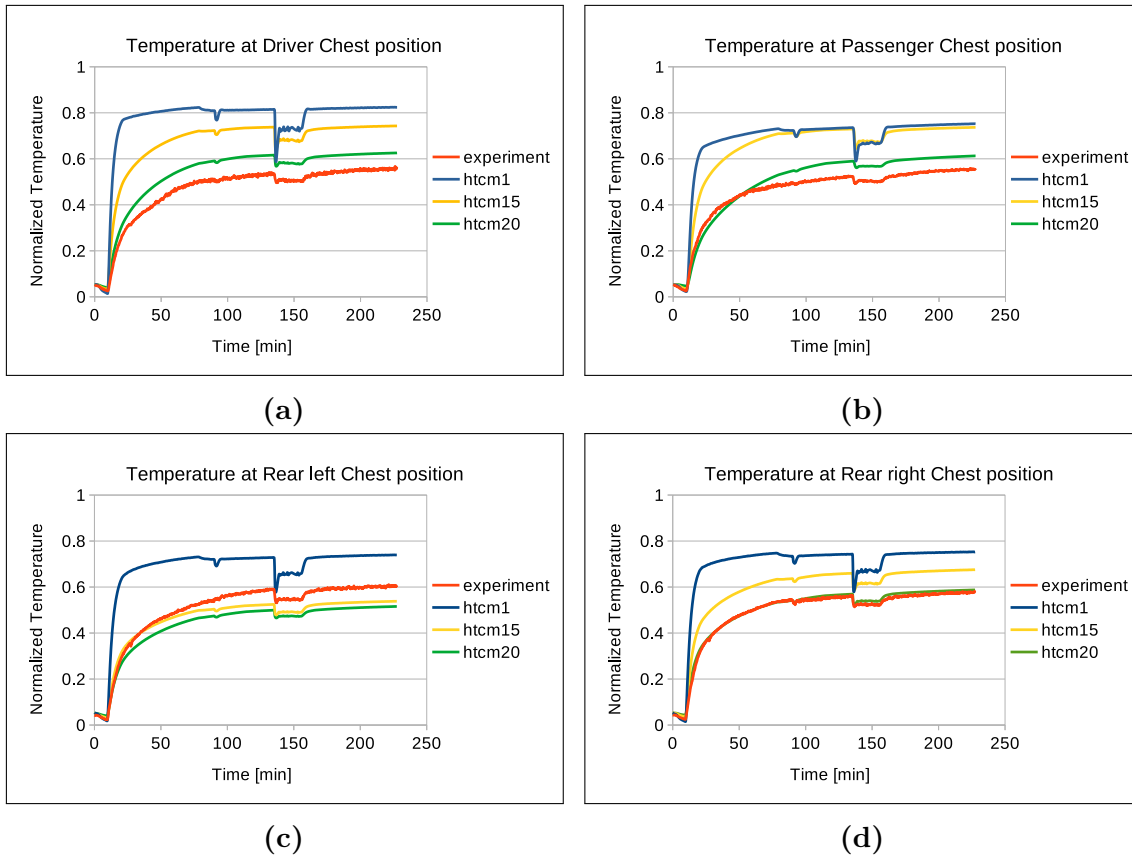


**Figure 4.9:** Comparison of temperature curves from the experiment with the simulation model at the four chest positions in the cabin which are (a) Driver (b) Passenger (c) Rear left seat (d) Rear right seat

When the model is calibrated with HTCMs, the multiplication factor applied globally for every region in the model, meaning that the Heat Transfer Coefficients (HTC) calculated at every flow cube is scaled by the factor of 20 or 15 as mentioned during the simulation set up. If the HTCs are not captured well by the flow cubes in GT-Suite, then the temperature curves cannot be captured accurately irrespective of the multiplier being used. Figure 4.8a and 4.8b shows that the HTC is captured well near the driver head and driver foot regions, hence calibrating it by a factor of 20 captures the temperatures at those zones accurately as in the experiments.

Figure 4.10 shows the temperature curves at the four foot positions in the cabin. It can be seen that the temperature curves when HTCM is 15 is not much different from the temperature curves when HTCM of 20 is used. This implies that even if the HTCM is further increased, it will not affect the results, meaning that the test data could not be matched by varying the HTCM in this model. This is because the heat transfer has reached a point of convergence at those regions, i.e. the heat transfer is taking place at a maximum rate for the calculated HTCs by the GT-Flow solver.

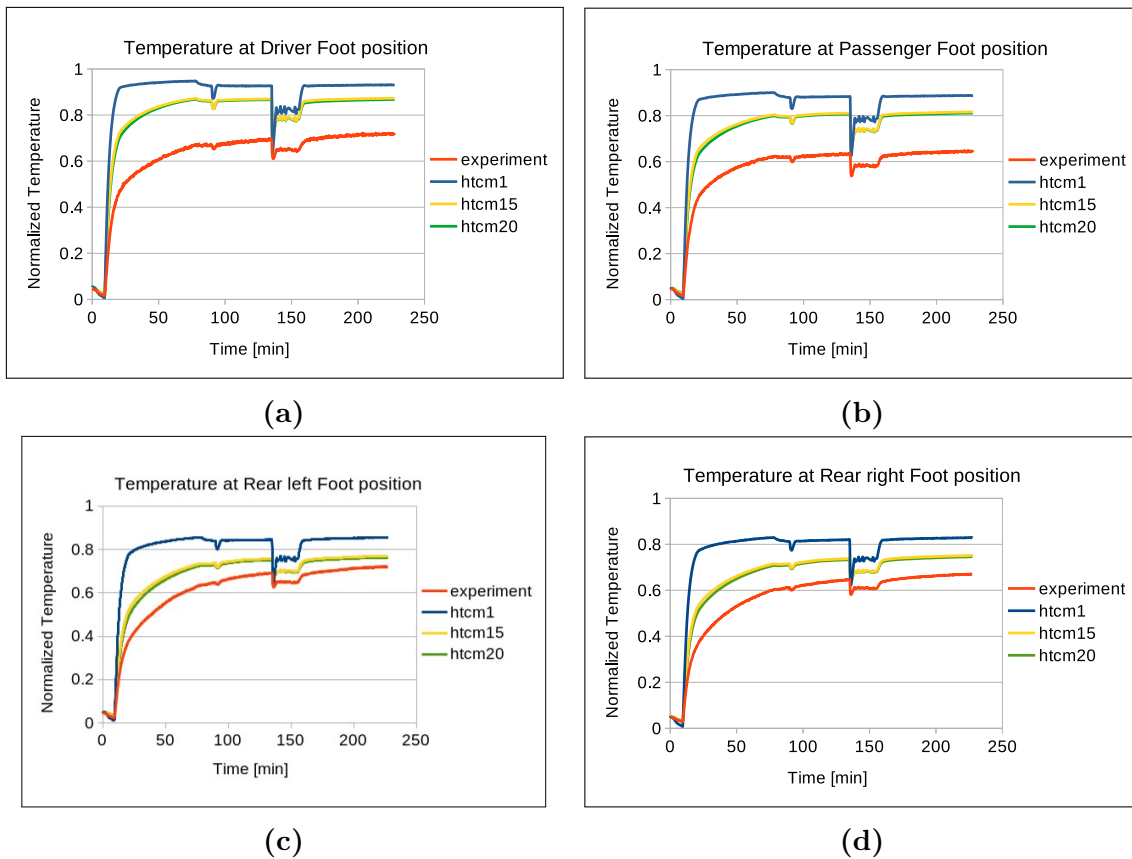


**Figure 4.10:** Comparison of temperature curves from the experiment with the simulation model at the four foot positions in the cabin which are (a) Driver (b) Passenger (c) Rear left seat (d) Rear right seat

Hence with this method, the local temperature at all the zones in the cabin cannot be captured accurately, mainly because the flow field distribution is not captured well by the flow cubes with leads to imprecise calculation of HTCs with GT-Flow Solution. Also, the flow cubes are quite large and are not able to account of the change in properties of the fluid within the volume of the cubes. To overcome this, a better method of capturing the flow fields and a better discretization needs to be implemented that would lead to better prediction of the HTCs in the cabin model.

### 4.2.3 Flow cube size variation

The results discussed in the above sections were computed for flow cubes of size 100x100x100 mm in the fluid domain discretized by COOL3D. In the GT-Flow solution, the recommended size of flow cubes is between 100 to 150 mm. To analyse the effect of the flow cube size in the end result, the fluid domain was discretized with two other flow cube size and the simulation was run with a HTC value of 20.

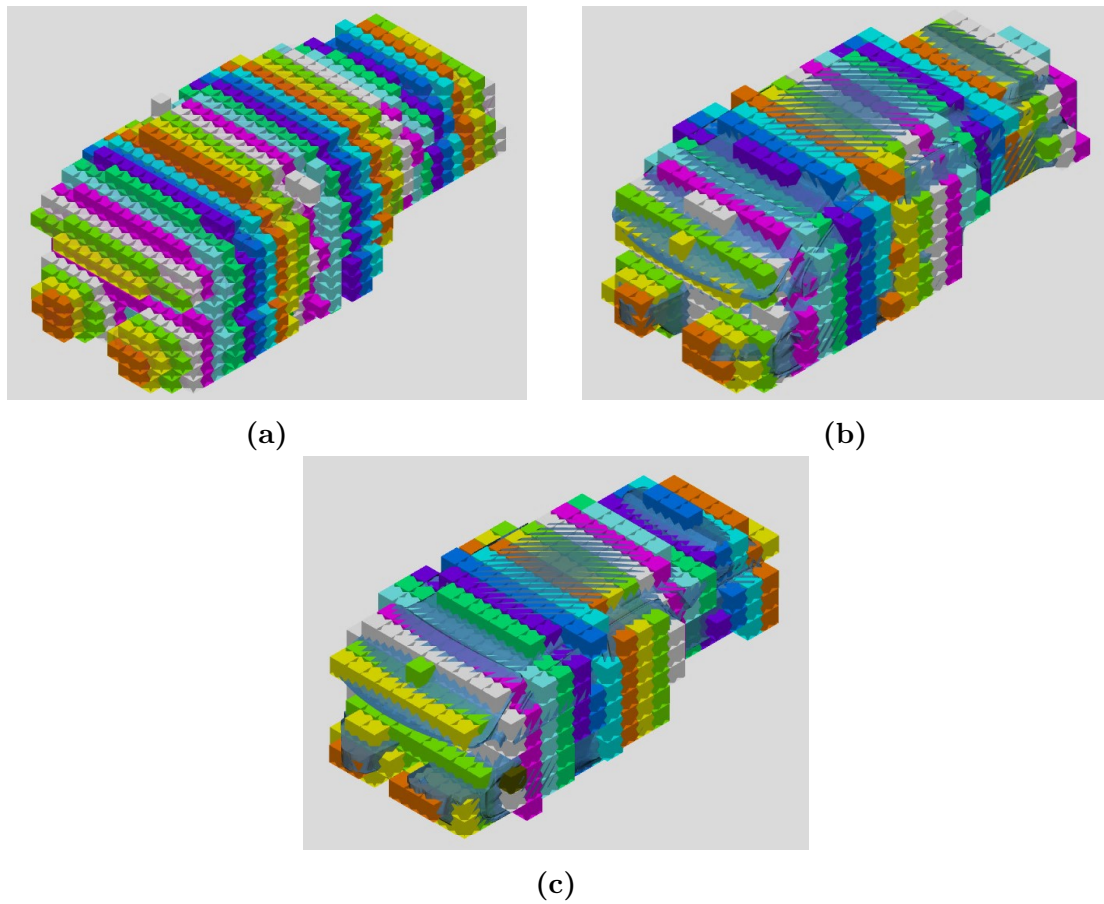


**Figure 4.11:** Discretized domain when flow cubes were set to (a) 100x100x100 mm (b) 130x130x130 mm (c) 150x150x150 mm

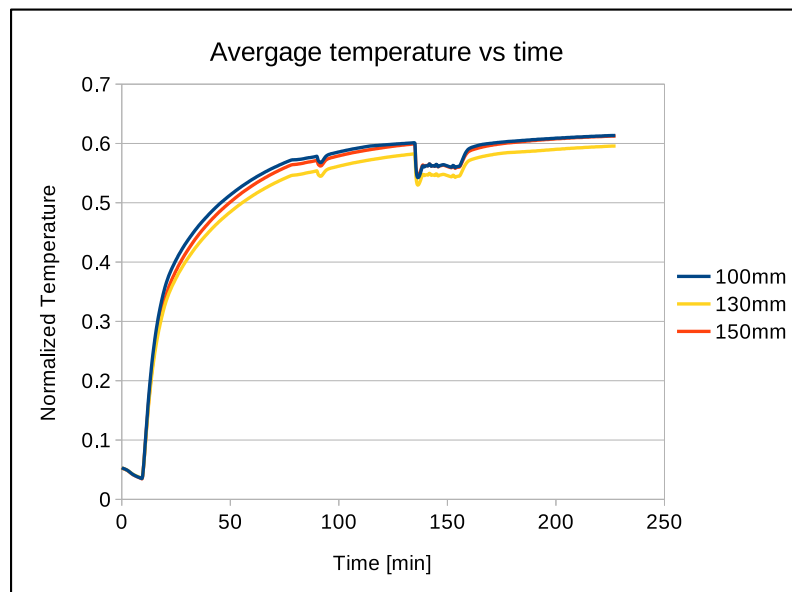


**Figure 4.12:** Average temperature recorded by all sensors in the model for a HTCM value of 20 for different flow cube sizes

The temperature curves for different flow cube sizes are shown in figure 4.12. The simulations were run for an HTC<sub>M</sub> value of 20 for all three flow cube sizes so that they can be compared. It can be seen that the change in the flow cube size does not affect the result to a large extent. This is because the solution with GT-Flow is an approximate solution that does not capture the flow fields accurately. Even with refining the fluid domain by having smaller flow cubes, the solver still behaves in a similar way and hence it is not recommended to reduce the flow cube size further to check if the results get better. Instead, CFD flow field mapping was used to capture the flow fields, which is discussed more in the following sections.

### 4.3 GT Solution with CFD flow field mapping

For better flow field resolution, CFD flow field mapping method is recommended. This section discusses the results obtained from the co-simulation setup when CFD results from steady simulations were mapped with the co-simulation interface. This involves running one steady state simulations for every fan speed, using the CFD mesh data for better discretization in COOL3D and the CFD flow variables to capture the velocity field and HTC<sub>s</sub> during the co-simulation.

#### 4.3.1 3D CFD Maps

In the CFD flow field mapping method, a steady state simulation for the four different fan speeds was done before setting up for the co-simulation. The model parameters for this simulation was discussed in section 3.2.1 in the methods chapter. The mass flow rate and temperature of air entering the cabin through the vents were recorded and given as inlet boundary conditions in these steady state simulations.



**Figure 4.13:** Velocity contour plot at the vent cross section when fan speed was set to level 1

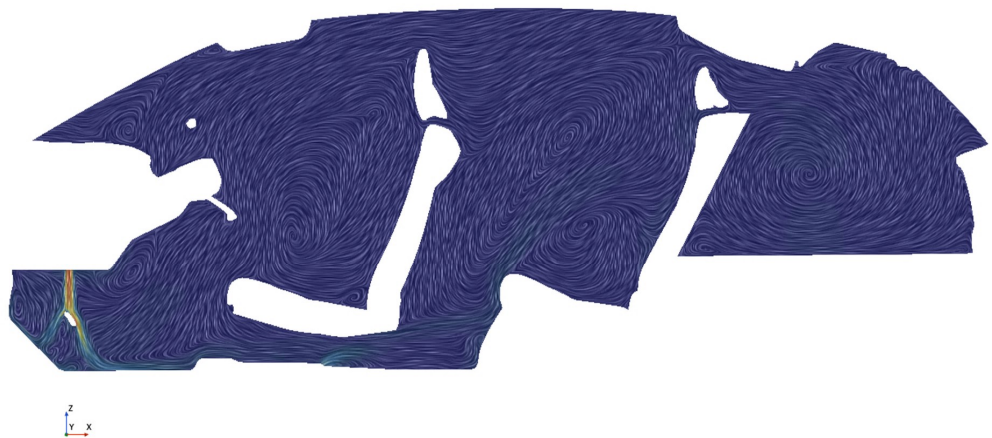


**Figure 4.14:** Velocity contour plot at the vent cross section when fan speed was set to level 2

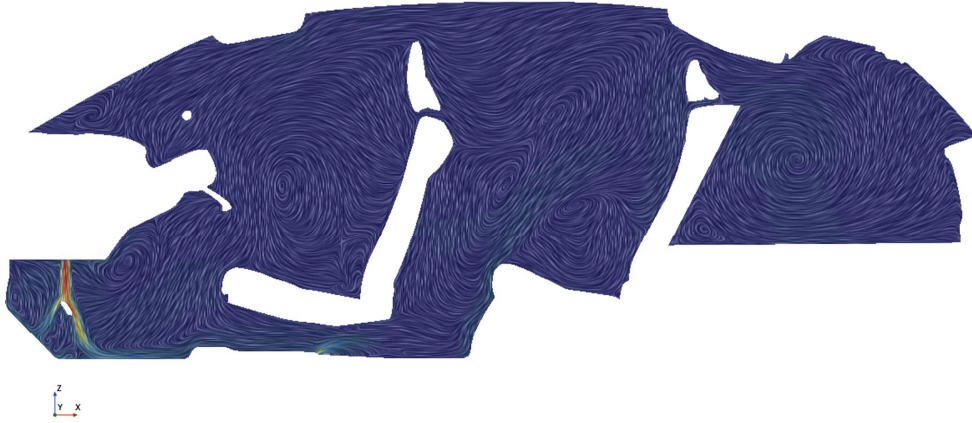


**Figure 4.15:** Velocity contour plot at the vent cross section when fan speed was set to level 3

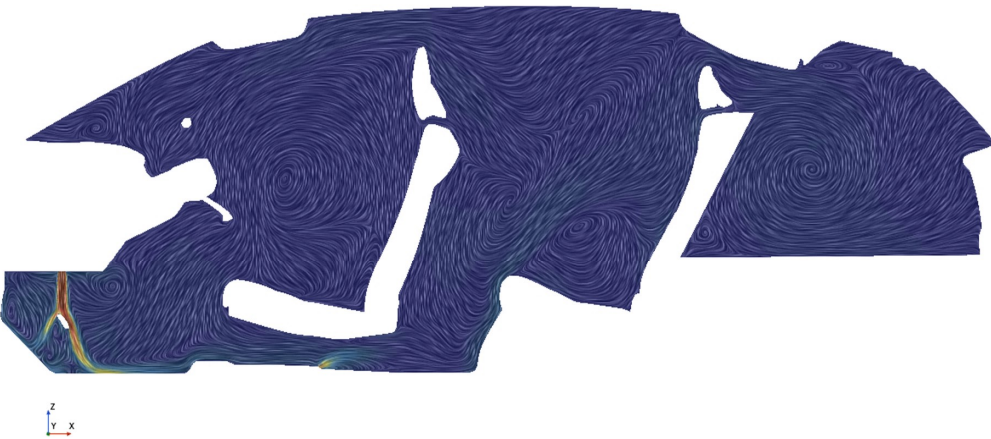


**Figure 4.16:** Velocity contour plot at the vent cross section when fan speed was set to level 4

Figures 4.13, 4.14, 4.15 and 4.16 shows the velocity contour plots for the four steady state simulations that were performed for the purpose of mapping the CFD data into the co-simulation. The scale of the graph has been removed in order to protect the sensitive data. These contours give the velocity distribution in a cross-sectional plane to which the normal is along the y-direction. The cross-sectional plane is taken at the middle of the driver seat in order to illustrate the flow velocity of air entering the cabin through the foot vent at the driver position. The plots have been scaled to the same range so that they can be compared to each other. As expected, the simulation with fan speed level 4, which operates at the highest RPM, has higher velocity of air entering the cabin through the four foot vents shown in figure 4.16. The data from these steady state simulations were exported into the co-simulation interface in GT-ISE once convergence was achieved in the steady state simulations

### 4.3.2 Results with 3D CFD Mapping

Using the steady state simulation results, the co-simulation with CFD flow field mapping was performed. The mesh data from Star CCM+ was used for discretizing the domain in COOL3D, hence a more finely discretized fluid domain was obtained for the co-simulation interface. This was followed by importing the CFD data into the system simulation interface which was discussed in detail in section 3.2.2. The results from the co-simulation with the CFD flow field mapping was compared with the experimental data. Since the flow field mapping method provides the option of running multiple fan speeds for the simulation, the simulation was run for the complete run involving all the four different fan speeds as done in the experiment. The temperature curves for all the 12 sensor positions and their average were compared with experimental data.

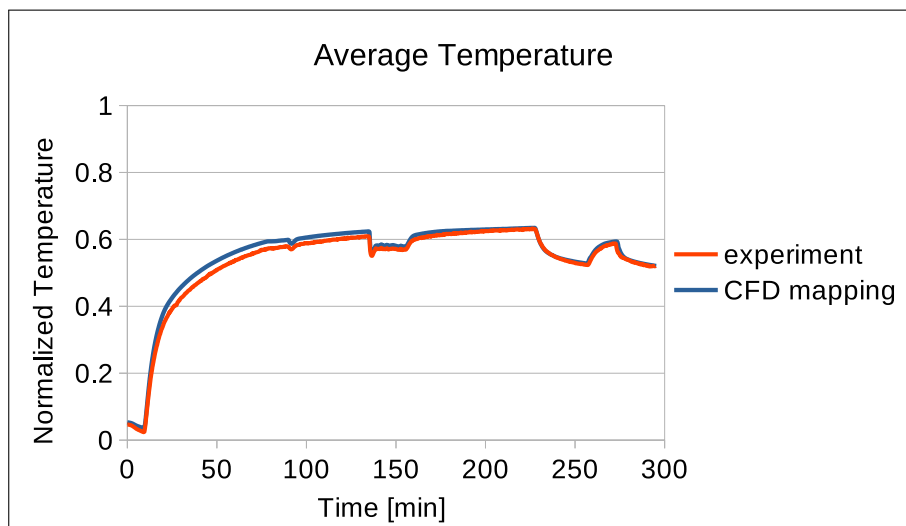


**Figure 4.17:** Average temperature recorded by all the 12 sensors placed in the cabin in experiments and simulation model

## 4. Results and Discussion

Figure 4.17 shows the temperature curve for the average of all the sensors that recorded the temperature in the experiment and the model that used CFD mapping. As seen in the figure, the simulation result agrees well with the experimental result. The method does not require any calibration and can still produce the results accurately as the HTC's are computed by Star CCM+ which are more precise. To analyse how well the temperature is captured at each zone in the cabin, the data from all the 12 zones in the cabin compared with experimental data.

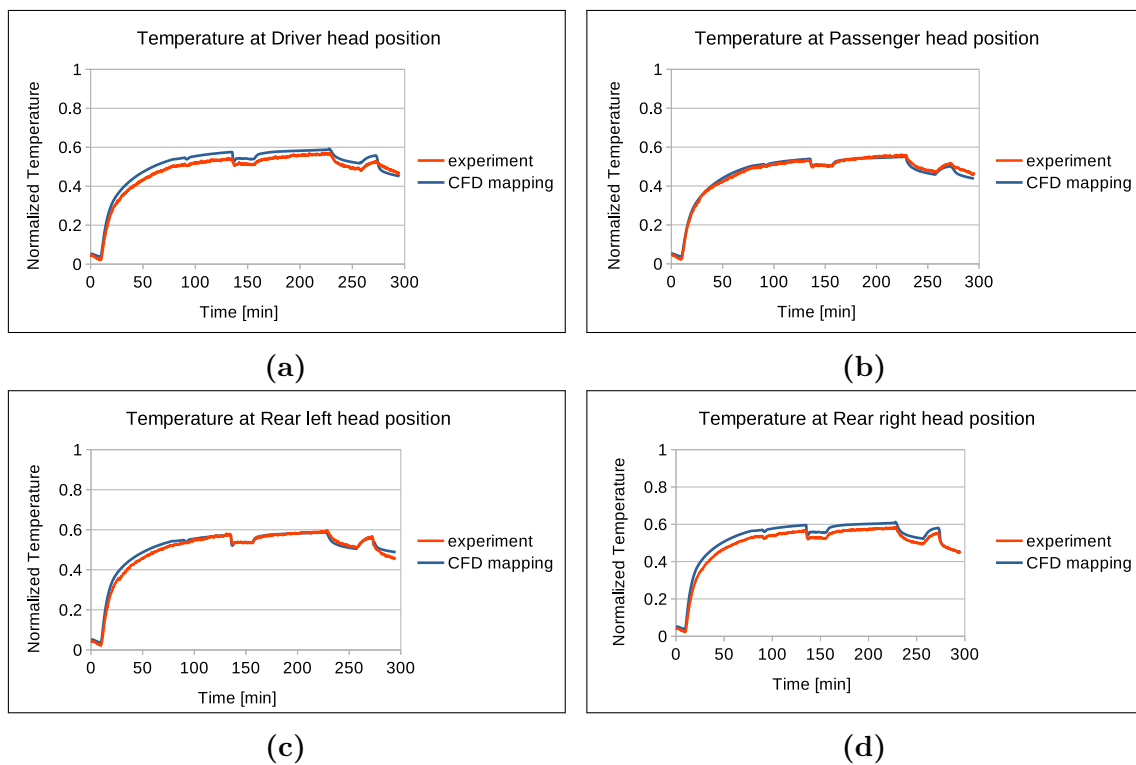


**Figure 4.18:** Comparison of temperature curves from the experiment with the simulation model at the four head positions in the cabin which are (a) Driver (b) Passenger (c) Rear left seat (d) Rear right seat

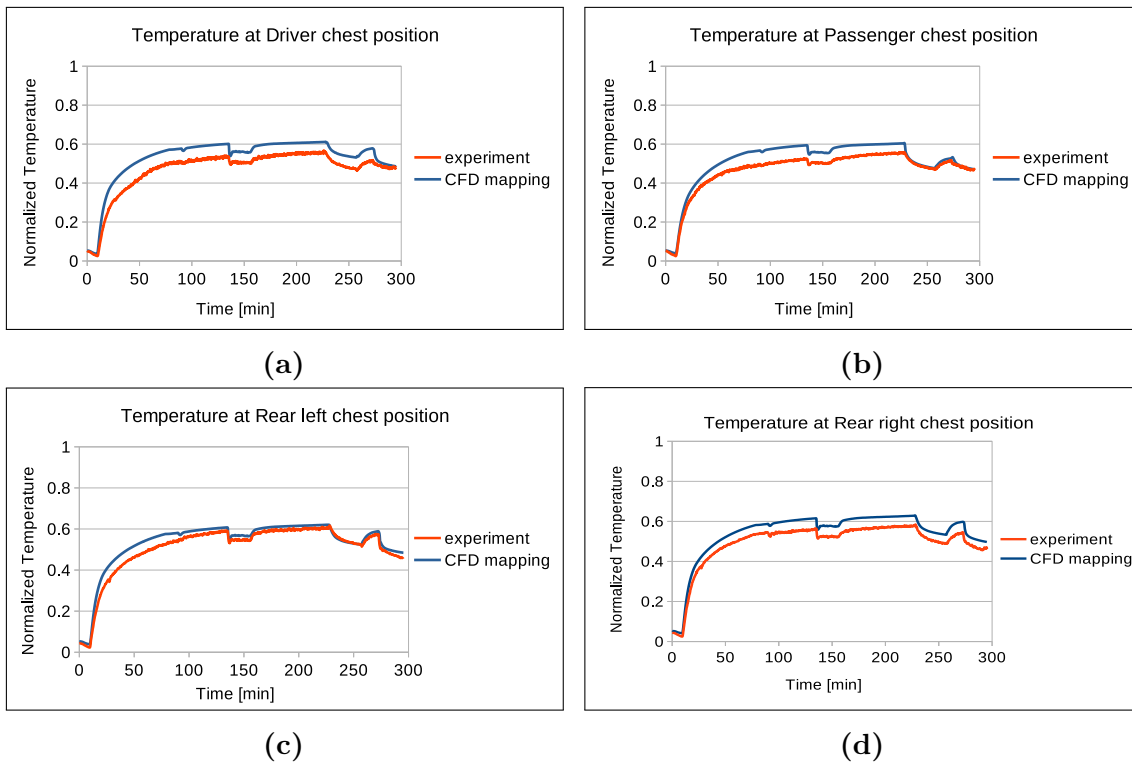


**Figure 4.19:** Comparison of temperature curves from the experiment with the simulation model at the four chest positions in the cabin which are (a) Driver (b) Passenger (c) Rear left seat (d) Rear right seat

Figure 4.18, 4.19 and 4.20 depicts the temperatures recorded the sensors in the experiments and simulation in the head, chest and foot regions respectively. The CFD mapping method has proved to capture the temperatures at each zone with better accuracy, as the simulation curves lie close to the experimental curves.

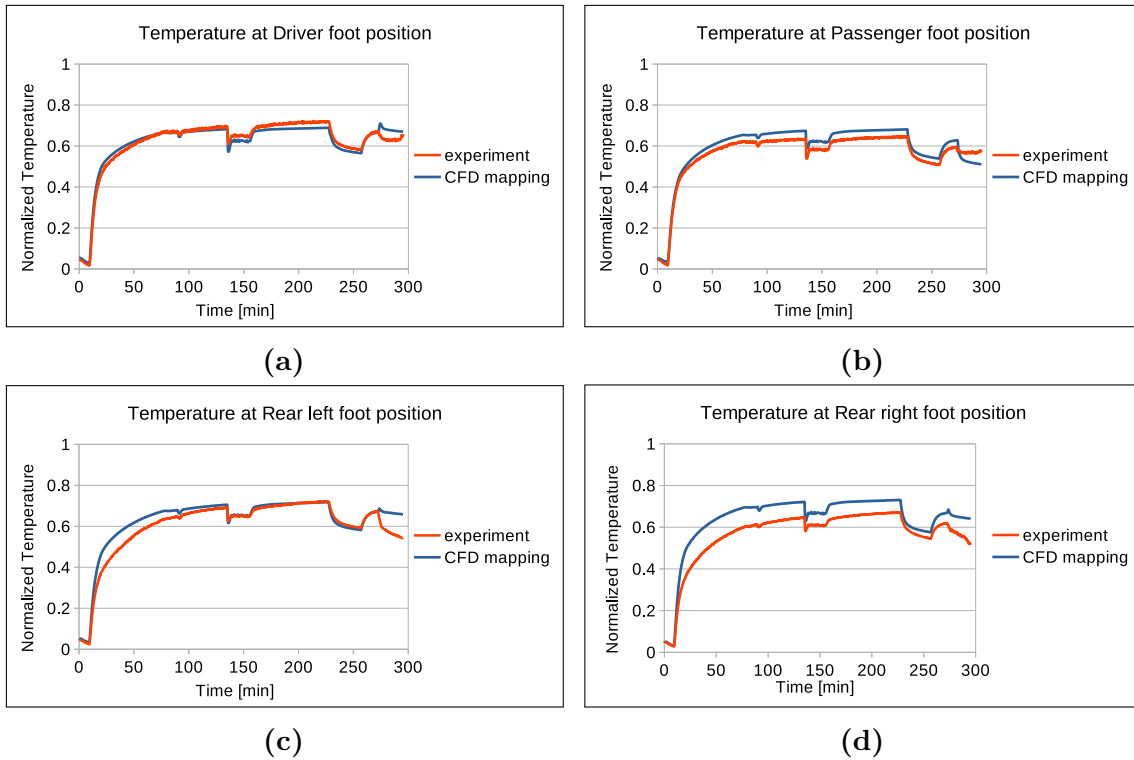


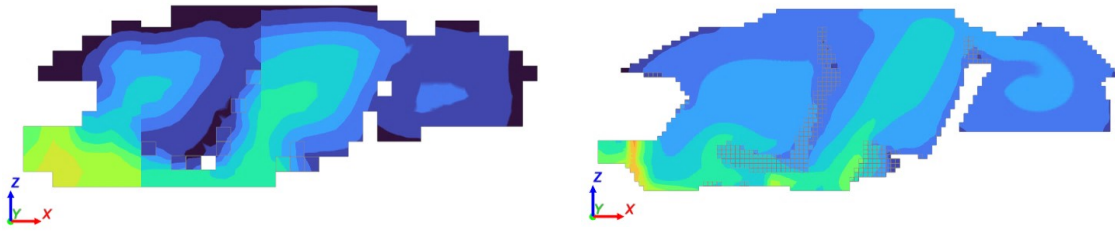
**Figure 4.20:** Comparison of temperature curves from the experiment with the simulation model at the four foot positions in the cabin which are (a) Driver (b) Passenger (c) Rear left seat (d) Rear right seat

## 4.4 Comparison of GT-Flow Solution and CFD Mapping Solution

The results from the co-simulation with both methods were discussed in detail in the previous sections. From the results, it is evident that the results from the CFD flow field mapping simulation is much better compared to the GT-Flow Solution in terms of capturing the temperature curves accurately without the need for calibration at every zone in the cabin model. It is interesting to see the temperature distribution in the cabin with both methods and how much time the co-simulation solver takes to run the complete simulation. These aspects are discussed in this section.

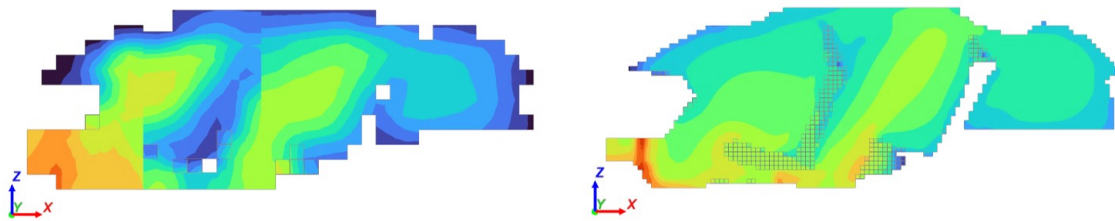
### 4.4.1 Temperature distribution

The main reason why the CFD flow field mapping method is able to capture the temperatures at each zone accurately accounts to the fact that the temperature distribution throughout the cabin is solved with better accuracy. Since the flow field is solved in Star CCM+, the HTC's are calculated with better precision leading to better temperature distribution. It also stems from the fact that when CFD mesh data is used for the flow cubes are discretized to size of 30x30x30 mm cubes which is much better resolution compared to the flow cubes of size 100x100x100 mm used in GT-Flow solution.



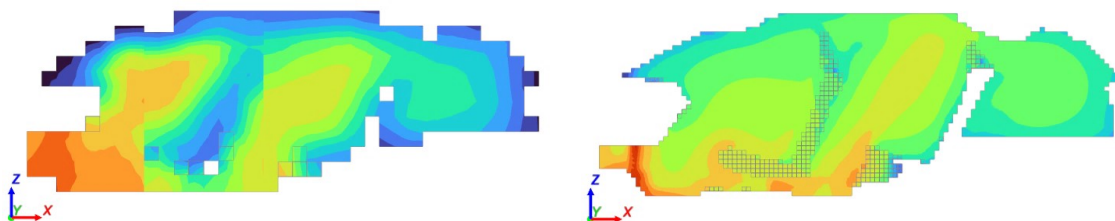
(a) GT-Flow Solution with HTC of 20      (b) CFD flow field mapping solution

**Figure 4.21:** Temperature contours in the cabin cross sectional area after 15 minutes of simulation time



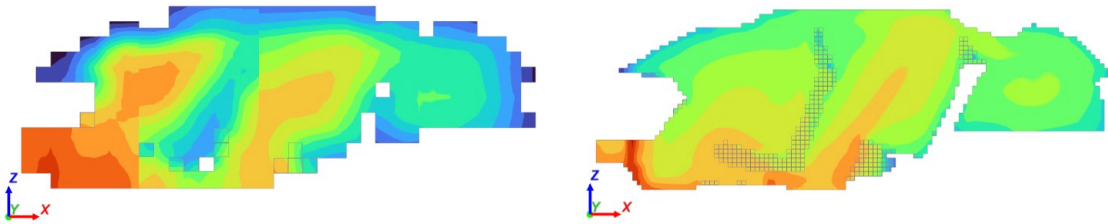
(a) GT-Flow Solution with HTC of 20      (b) CFD flow field mapping solution

**Figure 4.22:** Temperature contours in the cabin cross sectional area after 30 minutes of simulation time



(a) GT-Flow Solution with HTC of 20      (b) CFD flow field mapping solution

**Figure 4.23:** Temperature contours in the cabin cross sectional area after 45 minutes of simulation time



(a) GT-Flow Solution with HTC of 20      (b) CFD flow field mapping solution

**Figure 4.24:** Temperature contours in the cabin cross sectional area after 60 minutes of simulation time

The figures illustrated above show the temperature contours obtained from the simulation after a simulation duration of 15, 30, 45 and 60 minutes. The simulation where HTC of 20 was used, was the closest to experiments in GT-Flow solution method. Hence those results were compared to the results obtained from CFD flow field mapping method.

It is evident that GT-Flow Solution gives results with high temperature gradients throughout the cabin. The temperature close to the roof is very much lower than the temperature at the foot. This is because of the large flow cubes and poor flow resolution associated with the GT-Flow Solution method. Whereas, when CFD flow field mapping is employed, the temperature distribution is more uniform leading to smaller temperature gradients throughout the cabin volume as it occurs in experiment. Hence the temperatures at each zone are captured better in this method and it is evident from the results discussed in section 4.3.2.

#### 4.4.2 Computational time

This method of cabin simulation was developed with the idea of saving computational time compared to a full 3D transient simulation with any CFD simulation software. So, it is of interest to see the time taken for the solver to compute the results for the simulation. Since the simulations with GT-Flow Solution was computed for 227 minutes for one fan speed, the computational time for the simulation of first 227 minutes for the CFD mapping method was compared with the computational time taken by the simulations with GT-Flow Solution.

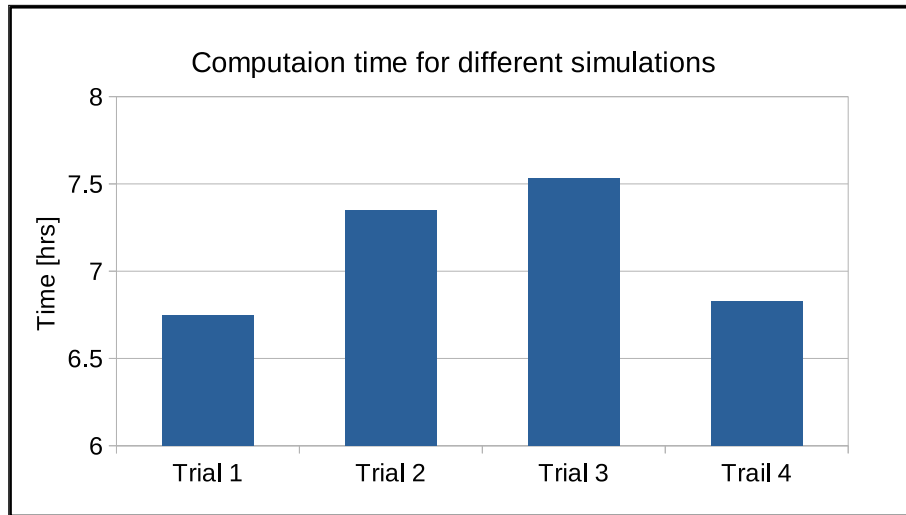


**Figure 4.25:** Computational time for the different simulations

Trial	Description
1	GT-Flow Solution without calibration, i.e. $HTCM = 1$
2	GT-Flow Solution with calibration of $HTCM = 15$
3	GT-Flow Solution with calibration of $HTCM = 20$
4	CFD flow field mapping solution

**Table 4.2:** Description of the simulations for which the computational time was compared

When comparing the different simulations in GT-Flow Solution method, it can be seen the computational time for the simulation increases when the HTCM increases. This implies when the HTC is scaled up enabling more heat transfer between the wall structures modelled in TAITherm and fluid domain modelled in GT-Suite, the solver takes more time to reach a steady solution at each time step causing more time for computation. Hence, a trend of increasing computation time with increasing HTCM can be observed.

The computational time for the simulation using CFD flow field mapping takes around 6 hours and 50 minutes for a simulation duration of 227 minutes (3 hours and 27 minutes). It must be noted that this is the time taken by the co-simulation once the steady state solutions were mapped on to it. The computational time for the different steady state simulation may vary depending on the number of cores used for running the simulation, meshing strategy, inlet boundary conditions, physics models chosen, etc. By only comparing the computation time for the co-simulation for the CFD flow field mapping solution, it was around twice the simulation duration which is much lesser than the time taken by a full transient 3D CFD simulation.



# 5

## Conclusion

To conclude, the thermal cabin model was developed and the solution with GT-Flow and CFD flow field mapping methods were studied. It was evident that the CFD flow field mapping method was more accurate and agreed with the test results well in all the regions in the cabin. This was because the velocity field and the HTC's were computed by the 3D CFD software Star CCM+ which led to more accurate results. However, the GT-Flow Solution can still be used if the temperature of only one zone in the cabin is of interest. In that case, the model heavily relies on the experimental data for calibration.

The current cabin model that is being used at Volvo Cars is a low-fidelity 1D model built with GT-Suite that requires a lot of manual calibration and does not capture the local temperatures that well. The model developed with the GT-Flow Solution method was able to capture the temperatures at certain zones well with some calibration, but not so well in other zones, in spite of calibrating the data. But the model that uses CFD flow field mapping proved to be a more accurate and a high-fidelity model whose benefits seems to outweigh the cost associated with it. This method of cabin model development has given promising results and maybe be investigated further.



# 6

## Future works

The objective of the thesis was to develop a cabin thermal model that can predict the temperature inside the cabin for any type of configuration. Even though this was achieved, there are a few aspects that can be included in the model to investigate the robustness and flexibility of this method of cabin modelling.

The cabin model developed was tested for a heat-up simulation in this thesis. When CFD flow field mapping method was used, the results from the simulation agreed well with the experiments. When GT-Flow Solution was tested the simulation with HTC<sub>M</sub> of 20 was the closest to the experiments. It would be interesting to perform a cool down test, i.e. place the cabin in a hot ambient condition and pump cold air in the cabin to cool it down. The same can be simulated and the HTC<sub>M</sub> required for that condition can be analysed to see how much it varies from the one used in the heat-up simulation.

Increasing the communication interval reduces the computational time in this model. The communication interval can be increased further until it starts affecting the results by causing instabilities, in an effort to reduce the time taken for the simulation to run.

The presence of passengers inside the cabin can have an effect on the cabin temperature as the human bodies can act as thermal masses, affecting the heat transfer inside the cabin. TAItherm has feature of including a human mannequin model in the cabin which would include the bone, tissue, skin and cloth models. This can be introduced in the co-simulation model to study its effects.

As the multi-layered model is a weighted average model of the whole vehicle, the results can be made more accurate by improving how the weighted averaging is done. Since the conductivity depends on series or parallel arrangements, including this during the averaging process can give an even better model.



# Bibliography

- [1] Theodore L Bergman et al. *Fundamentals of heat and mass transfer*. John Wiley & Sons, 2011.
- [2] Christoph Boettcher and J Wiedemann. “Simulation of a passenger car cabin using a coupled GT-SUITE-TAITHerm simulation model”. In: *University of Stuttgart* (2016).
- [3] Lars Davidson. *Fluid mechanics, turbulent flow and turbulence modeling*. 2015.
- [4] Jalal Jalil. “CFD Simulation for a Road Vehicle Cabin”. In: *journal of King Abdulaziz University Engineering Sciences* 18 (Jan. 2007), pp. 129–148. DOI: 10.4197/Eng.18-2.7.
- [5] Jonas Jonsson. “Including solar load in CFD analysis of temperature distribution in a car passenger compartment”. In: (2007). Validerat; 20101217 (root).
- [6] Ola Löseth. “Development and optimization of climate-and energy related models in electromobility using thermal comfort and CFD”. In: (2022).
- [7] Gamma Technologies. “3D cabin modeling tutorials”. In: (2022).
- [8] HK Versteeg and W Malalasekera. “Computational fluid dynamics: the finite volume method”. In: *Harlow, England: Longman Scientific & Technical* (1995).



DEPARTMENT OF SOME SUBJECT OR TECHNOLOGY  
CHALMERS UNIVERSITY OF TECHNOLOGY  
Gothenburg, Sweden  
[www.chalmers.se](http://www.chalmers.se)



**CHALMERS**  
UNIVERSITY OF TECHNOLOGY